國立交通大學

光電系統研究所

碩士論文

具奈米線-聚塞吩網絡之複合式薄膜電晶體

Hybrid Thin-Film Transistors Based on Nanocomposite Silicon Nanowire and Polythiophene Networks

研究生：鄭光耀

指導教授：謝建文 博士

中華民國一百零二年十一月

具奈米線-聚塞吩網絡之複合式薄膜電晶體

Hybrid Thin-Film Transistors Based on Nanocomposite Silicon Nanowire and Polythiophene Networks

研究生：鄭光耀　　Student：Kuang-Yao Cheng

指導教授：謝建文　　Advisor：Chien-Wen Hsieh

國立交通大學

光電系統研究所

碩士論文

A Thesis

Submitted to Institute of Photonic System

College of Photonics

National Chiao Tung University

in partial Fulfillment of the Requirements

for the Degree of

Master

in

Photonic System

November 2013

Tainan, Taiwan, Republic of China

中華民國一百零二年十一月

具奈米線-聚塞吩網絡之複合式薄膜電晶體

研究生：鄭光耀　　指導教授：謝建文 博士

國立交通大學

光電系統研究所碩士班

摘要

有機半導體材料因為在發光二極體、太陽能電池、電子紙，射頻識別標籤的應用範圍具有極大潛力而備受關注。所有這些電子產品都可以用非常低的成本、較低的製程溫度，且很容易地利用大面積製造技術應用在可撓性基板上。具有較高的場效應載子遷移率和適於溶液態操作特性的共軛高分子半導體（例如，區域規則性聚塞吩）已被應用在有機薄膜電晶體中。由於有機薄膜電晶體的性能與聚合物薄膜的結構排列息息相關，可用於溶液化製程的自組裝區域規則性聚-3-己基塞吩（P3HT），具有顯著擇優取向的有序結構，使得共軛平面垂直於基材表面，而這似乎非常有助於載子傳輸，P3HT 因此也成為最受矚目的材料之一。然而儘管材料的功能和處理技術有最新的進展，有機薄膜電晶體的元件壽命和載子遷移率，使得它在更廣範圍的應用上仍然受到限制。本論文研究一種具有機半導體和平行排列的奈米線網絡的複合式薄膜電晶體，利用最近發展的拉伸接觸轉印技術將

奈米線陣列，整合於旋轉塗佈的半導體高分子層下，形成如奈米複合材料的主動通道來進行載子傳輸。與單純有機高分子元件相比，此複合式薄膜電晶體在載子遷移率(提高到四倍)和空氣中穩定性上達到正向提升的作用。

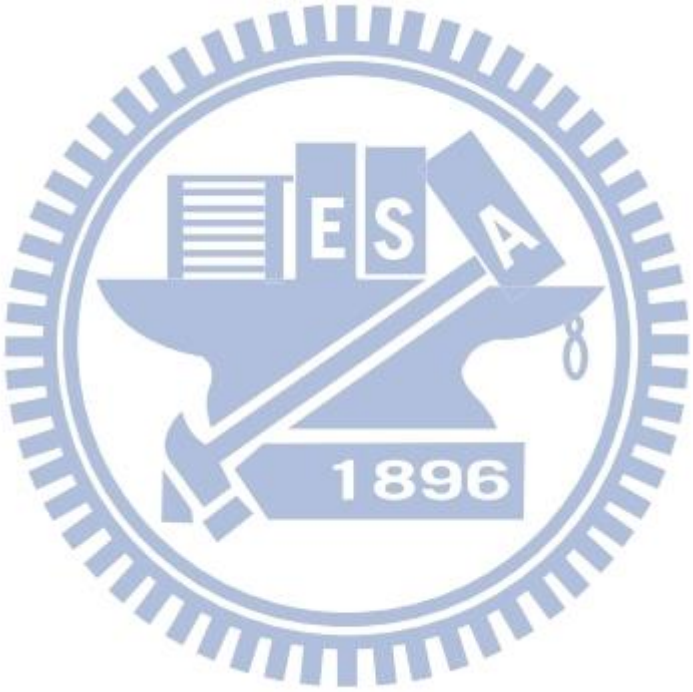

Hybrid Thin-Film Transistors Based on Nanocomposite P3HT and Silicon Nanowire Networks

Student : Kuang-Yao Cheng Advisor : Dr. Chien-Wen Hsieh

Institute of Photonic System

National Chiao Tung University

Abstract

Semiconducting organic materials have their great potential in applications ranging from, solar cells, LED, RFID tags, and E-papers. It can realize large area fabrication on flexible substrate at low cost. Conjugated semiconducting polymers with high carrier mobility and solution process ability characteristics (e.g., regioregular polythiophene) have been introduced into the fabrication process of organic thin film transistors (OTFTs). Since the OTFTs performance strongly depends on the structural arrangement and ordered orientation of π-conjugated planes perpendicular to the substrate surface of the polymer thin film. Self-organized regioregular poly-3-hexylthiophene (rr-P3HT) has above favorable properties which seem to be very helpful in carrier transport and also has remarkable solution process ability. Despite recent advancements in material functionality and processing technologies, OTFTs are somewhat limited in terms of device lifetime and mobility, which hinder their adoption on a wider scale. This work demonstrated a series of hybrid thin film transistors (TFTs) with a network of organic semiconductors and parallel aligned nanowires. Silicon nanowire arrays, assembled by a recently developed stretched contact printing technique, are embedded in a layer of a spun-coat semiconducting polymer, forming a nanocomposite active channel for electrical conduction. The hybrid

TFTs have revealed an enhancement in charge carrier mobility (up to four times) and air stability compared to those of the pristine polymer host.

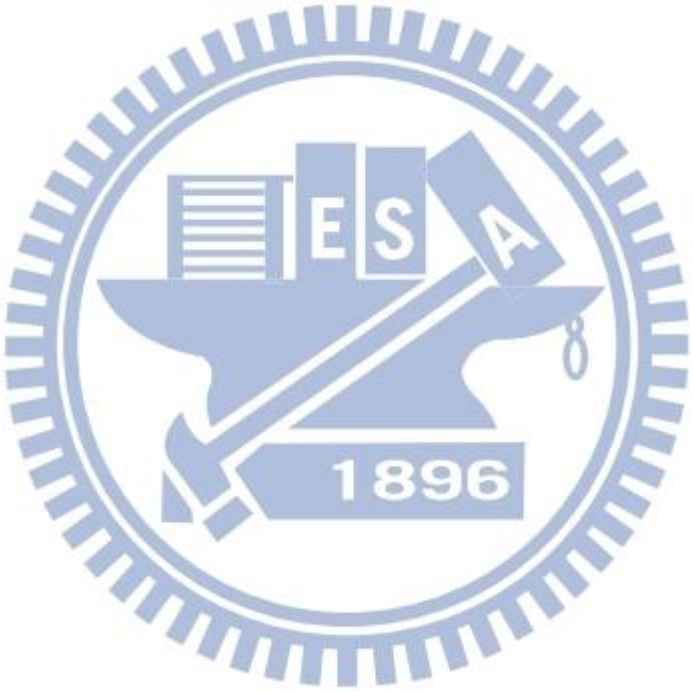

Acknowledgement（致謝）

現在都還記得當初考上研究所和指導教授在圖書館面試的場景，一轉眼已經過了兩年半的時間了，實驗室從空無一物的房間，到能夠做出實驗結果、參加研討會，雖然很遺憾地沒有辦法在碩士班當中發表期刊、參加國外研討會、得一些獎項來增加實驗室光彩，但是這兩年所學到的經驗和知識卻是非常飽滿的。努力並不一定會有收穫，但是不努力就很難有收穫，作為本實驗第一屆第一位的畢業生，其實很多事情到現在都還是很懵懂的，研究所很難有人會按部就班的指導你，特別是在沒有學長姐的情況下，感謝謝 建文教授的努力，我們才能夠順利的進行實驗，讓實驗室從無到有，想必教授也是非常辛勞。

在實驗期間我必須感謝實驗室的同學 家源磨練我的耐心，以及實驗室學弟妹世平、彥升、齡誼的協助，另外一路領導我給我寶貴意見的郭政煌老師實驗室的力權學長和劉家明老師實驗室的仕賢學長，讓我受益良多。楊勝雄老師實驗室的維勝、國兼、子軒在煩悶的日子裡帶來歡笑、蘇海清老師實驗室的柏村、元配、阿昇、櫻桃、瑞哥在實驗上的相互協助、籃球場上的熱血都讓我相當難忘。碩一上的 417 共同實驗室的夥伴們，直到現在都還很懷念和你們一起念書一起玩的日子。台南應用科技大學的蘇西、思思、小綠、加加、欣欣、凡凡也因為你們我多了點藝術氣息。陪我撐到最後的林萬里老師實驗室的赤唐和鄭協昌老師實驗室的台客。這些日子陪

我排憂解悶的小鬼和健文。在我進研究所之前就給我許多震撼教育的力王，以及常常跟我分享心情的老盧。

感謝願意讓我走入他的世界的白白，以及她的好姊妹們；千雅、麗娟、珊珊、球球、大隻、泰安，因為有了妳，我的世界開始變得不一樣，雖然研究所曲曲折折，但是結局還是很美好，最後我要感謝我的父母和家人，如果沒有你們就沒有我，你們一路的支持和體諒是我前進最大的動力，

寫到這裡，我還是有很多想要感謝的人，雖然沒有在這篇致謝提到你(妳)，你們對我的幫助、對我的好我都會記在心裡的，謝謝你們因為有你們我的研究所生涯才能如此豐富，來台南念交通大學光電研究所這一趟，實在是不虛此行。

Table of Contents

Figure Captions

Chapter 1 Introduction

Chapter 2 Literature Review

Chapter 3 Experimental procedures

Table Captions

Chapter 1

Introduction

1.1 General Background

1930 Lilienfeld have proposed the idea of field-effect transistors (FET) [1], and written in the patent, but he has no actual experiment. Until 1947, W. Shockley, J. Bardeen, W. H. Brattain was actually made well known JEFT, and in 1956 received the Nobel Prize [2]. Then, in 1960 Kahng and Atalla made the first metal-oxide-semiconductor (MOS) transistor, the widely used MOSFET [3]. The development of organic semiconductors must to mention that Shirakawa contribution of the conductive polymer in 1977. The development is such a breakthrough so that he got the Nobel Prize in 2000 [4]. To be in 1986 by Mitsubishi Electric corporation Koezuka team made out of polythiophene FET, thus opening up the development of today's OTFT [5]. In just twenty years, this field has made rapid development. For example, the thin film transistor mobility from the initial 10^{-6} ~ 10^{-5} $cm^2V^{-1}s^{-1}$ rise to 10.0 $cm^2V^{-1}s^{-1}$ [6-8], an increase of over six orders of magnitude, the mobility of the organic crystal is more than 40.0 $cm^2V^{-1}s^{-1}$ [9-10]. Organic thin film transistor (OTFTs) driven displays, electronic paper, RFID tags and other products are gradually coming into view. These notices OTFTs have broad application prospects. There are many kinds of OTFTs material source. Controlling semiconductor performance can be achieved through molecular design and synthesis. It has good flexibility that can achieve full flexible devices and circuits which can be applied to the rollable

product such as electronic paper. (see in Fig.1-1). In addition, most OTFTs materials can be dissolved in common solvent, which can be used to solvent processing methods. For example: inkjet printing, spin coating, drop coating, micro-contact printing, etc., to prepare devices and circuits, thus promoting the development of printing electronics.

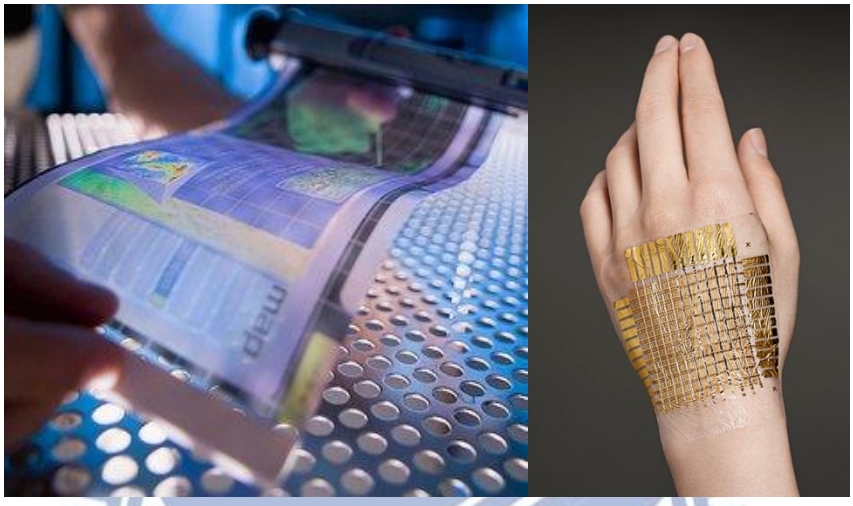

Fig.1-1 OFET-based flexible display [11] and electric skin sensor [12]

1.2 Operation principle of OTFTs

1.3 Motivation

OTFTs have much attraction by their solution process ability, low temperature processing, and potentially low cost fabrication, with the added advantage of lightweight, bendable features [13-14]. Despite recent advancements in material functionality and processing technologies, OTFTs are somewhat limited in terms of device lifetime and mobility, which hinder their adoption on a wider scale.

Recent progress on hybrid nanostructured inorganic-organic transistors may become an alternative means to conquer these barriers [15-16]. For instance, using carbon nanotubes as an additive into the organic-based semiconducting

channel has showed certain enhancement on device mobility due to their metallic/semiconducting electrical properties and unique one-dimensional structures [17]. Thus, further work on utilizing different nanostructures with high aspect-ratio into semiconducting organic hosts can help us disclose the potential of hybrid transistors [18].

The work centers on the hybrid nanowire-polymer semiconducting network for the generation of hybrid-based TFT devices. The network is consisted of a layer of parallel oriented silicon nanowires (Si NWs) and a subsequent organic layer of solution-processed poly-3-hexylthiophene, P3HT. The electrical characterization of these hybrid Si-P3HT TFTs and organic P3HT devices is investigated

1.4 Thesis Organization

This thesis is divided into five chapters. In Chapter 2, brief review active layer materials, transistor structure, and measurement and extraction methods of electrical parameters are introduced. In Chapter 3, the fabrication flow of hybrid OTFTs is described. In Chapter 4, electrical and material properties of devices are presented and discussed such as the Si-NWs density effect on hybrid OTFTs. Conclusions and future works are integrated in Chapter 5.

Chapter 2

Literature review

Chapter Overview

In section 2.1 of this chapter describes the operating modes and OTFT carrier transmission mechanism. In section 2.2 will review the promotion of organic and inorganic semiconductors arrangement method. In the organic semiconductor, a larger grain size, the smaller the grain boundary, and has a more orderly stacking direction, the transmission of the carrier has a positive impact. In the one dimensional composite material in transistors, highly directional, high-density structure of one dimensional materials show good improvement features, thus effective manufacture of high-density and high directivity one dimensional material structure also become a very important issue. This will introduce this experiment materials used in the active layer, and various control method of the organic semiconductor layer stack and the various effective permutation methods of the one dimensional material. In section 2.3 will briefly present hybrid OTFTs development, as well as the experimental materials used in the active layer. Section 2.4 is the literature review summary.

2.1 Structure and Theory of Organic Thin Film Transistors

OTFTs expected to be the basic building blocks for flexible integrated circuits and displays. A schematic structure in this thesis is shown in Fig. 2-1. The operation principle of FET that is to rely on a strong electric field induced current in the dielectric and semiconductor interface. By controlling the electric

field intensity to control source and drain current. To Bottom gate bottom contact structure as an example, insulating oxide layer spacing between the gate and the semiconductor, Source and drain contacts with the semiconductor. Source electrode injected the carrier flow to the channel. Channel current transport to the drain electrode. Professor Bao said ‘’For pixel switching transistors in liquid crystal displays, for instance, mobility greater than 0.1 $cm^2V^{-1}s^{-1}$ and ON/OFF ratio greater than 10^6 are needed [19].’’ In recent years, organic semiconductor materials have considerable progress on carrier mobility (see Fig. 2-2). Compared with inorganic semiconductor materials they still have much room for improvement (see Fig. 2-3). Hence, a variety of innovative ideas are constantly being proposed to hybrid materials based on inorganic and organic semiconductors may be one of the potential candidates.

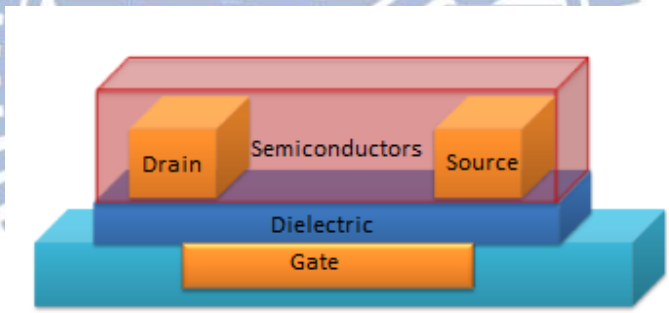

Fig. 2-1 Bottom gate bottom contact structure of an OTFT

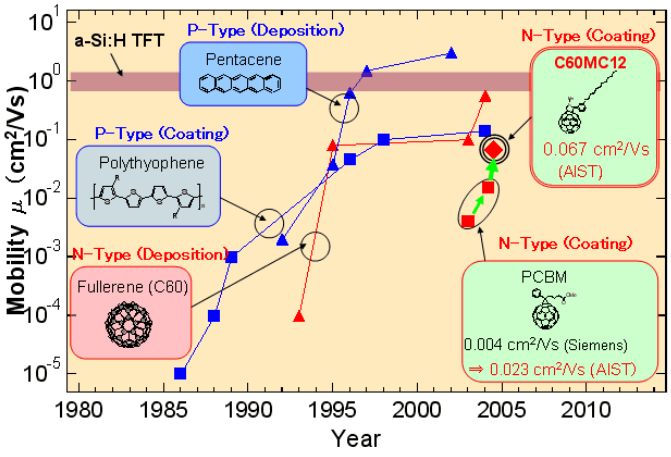

Fig. 2-2 Mobility of organic semiconductors [20]

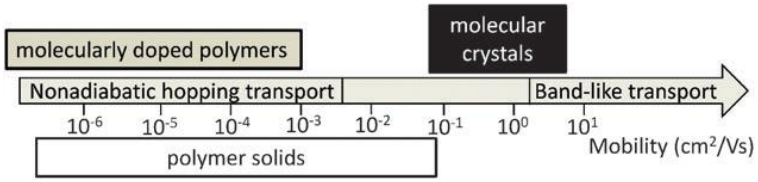

Fig. 2-3 The span of mobilities of organic materials of interest for electronic applications [21]

The π-bonding orbitals and quantum mechanical wave-function overlap are the most important mechanism for organic semiconductors charge transport [22]. Compared with high carrier mobility inorganic semiconductors, organic semiconductor molecular to form a grain is by weak Van de Waal force. Current carrier mean free path is less than the average distance between molecules, the degree of electron delocalization weaker than strong covalent bonding and inorganic semiconductors. Thus, developed a charge localization hopping transfer model which be called hopping model. Carriers were localized in a potential well. It need thermal excitation to assist to breakthrough the potential well, and overcome the energy barrier between two transition energy level to transport to the next potential well. Therefore, the charge transfer transition is thermally active. From microscopic view, carrier transition between molecule and molecule is continuous intermolecular redox process. This charge transport mechanism theory can be calculated by the famous Marcus theory [23]. Charge or hole carriers can use band-like transportation under external electric field (see Fig. 2-4). Carrier mobility is considered of the speed of many small energy level gaps for the holes or electrons to move between two energy levels. When the electric energy carriers continue toward the direction of high energy level, and have a short transition path, the carrier mobility will get higher [24].

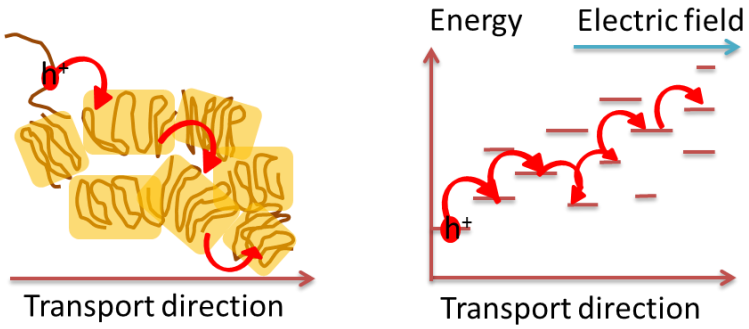

Fig. 2-4 Sketch of the spatial (left) and energy (right) landscape of hopping transport under the influence of an external electric field (redrew from ref. 21)

2.2 Semiconductor Material Alignment

2.2.1 Ordering of organic semiconductors

The carrier transport in OTFT is specific for two-dimensional carrier propagation through the device. Since the π-faces and the chain backbone are the only direction can transport charges (the side chains are insulators), the edge-on orientation has been suggested to benefit two-dimensional charge transport [25]. Therefore, for produce a transistors, a better arrangement of stacked, larger grain, smaller grain boundaries are needed. Besides, it hopes to be able to control lattice arrangement direction. Different arrangements have their advantages and disadvantages (see Table 2-1). The following are several methods to control polymer stacking direction：

(1) SAM treatment：Organosilanes such as alkylchlorosilanes, alkylalkoxysilanes, and alkylaminosilanes are the most widely used materials as effective surface modifiers because of the uniform and reproducible surface energy and hydrophobicity they provide (see Fig. 2-5a) [26-29].

(2) Solvent self-assembly：Polymer semiconductors easily dissolved in solvent, through use different solvents, mix different material (such as PMMA), use

various concentrations, to control the crystallographic orientation and crystallization characteristics (see Fig. 2-5b) [30-33].

(3) Electric field：Applying a strong electric filed during the thermal annealing process may be able to align molecules into a better crystal orientation (see Fig. 2-5c) [34].

(4) Substrate structure：Etching the substrate produce different density, aspect ratio of the groove, that crystal orientation can be effectively controlled (see Fig. 2-5d) [35].

(5) Alignment film：The concept is similar to the way of aligning liquid crystal. Using the alignment layer (such as PI), after rubbing method or photo-alignment method to achieve the effect of molecular alignment (see Fig. 2-5e) [36-37].

(6) Mechanical force：Using lateral sheared on the film or control the direction of fluid motion to have alignment of polymer film. Because external force is strong, so it is easy to have great impact on arrangement, but it is easy to destroy the film surface structure (see Fig. 2-5f) [38-40].

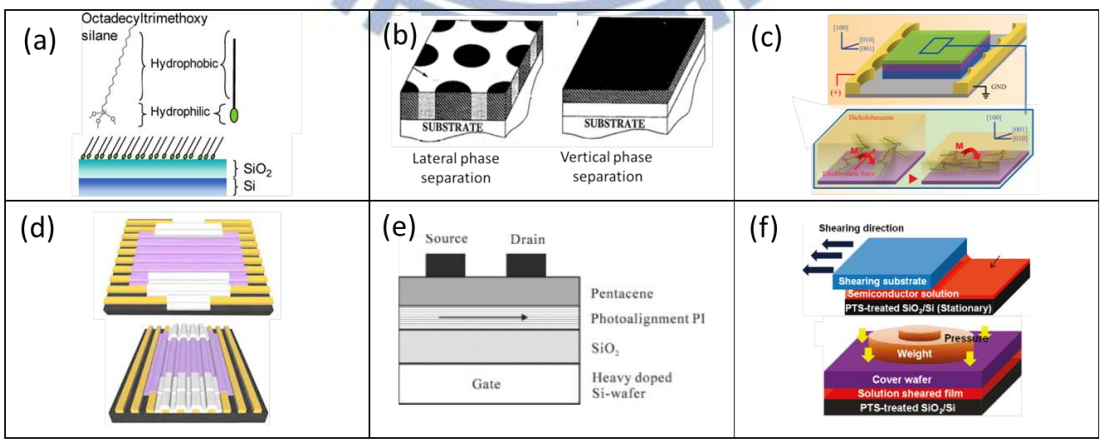

Fig. 2-5 Schematic view of molecular aligned methods. (a) SAM treatment [26] (b) Solvent self-assembly [33] (c)Electric field [34] (d) Substrate structure [35] (e)Alignment film [37] (f)Mechanical force [40]

Table 2-1 Comparison of alignment methods for organic semiconductors

Method	Advantage	Disadvantage
SAM treatment	It can change polymer face on to edge on.	It was unable to control the directionality of edge on phase.
Solvent self-assembly	It can be directly applied to the solution process.	Difficult in a large area with high directional effect.
Electric field	It can further increase in the thermal annealing properties of molecular arrangement.	The effect of arrangement is not significant. It was unable to effectively enhance carrier mobility.
Substrate structure	Applicable to various substrates and organic materials	Production process is more complicated. It is related to the structure aspect ratio and density.
Alignment film	An easy way to have alignment structure.	Alignment layer will affect the electrical properties.
Mechanical force	It has the ability to align molecular orientation very well.	There may be damage to the molecular structure, and will likely result in attachment or adhesion.

2.2.2 Assembly of 1-D nanostructures

For developed microelectronics, have high density, high directivity one dimensional material is very important things. Have good one-dimensional material properties and have effective to control density and direction are often able to demonstrate greater efficiency. Using 1-D nanomaterial with organic

materials also has been showed a good effect of improving. Here are some methods of transfer one dimensional material：

(1) Flow-assisted alignment：Use of air flow of controlling nanowire growth direction, to achieve the effect of nanowires arrangement (see Fig. 2-6a) [41-42].

(2) Deposition by chemical interactions：Use of surface treatment of one dimensional materials and substrate to get the effective arrangement (see Fig. 2-6b) [43].

(3) Langmuir—Blodgett technique：Pressure-induced isotropic-nematic-smectic phase transitions as well as transformation from monolayer to multilayer 1-D nanomaterial assembly. Then, use a surfactant to an aligned NWs layer on a surface of liquid, from where the NWs layer is transferred to a planar substrate (see Fig. 2-6c) [44-46]

(4) Blown-bubble technique：Use surface tension of bubbles blown to achieve one dimensional material array alignment, and transfer to the substrate (see Fig. 2-6d) [47].

(5) Electric field directed deposition：Use strong electric filed between adjacent electrodes to polarize and align the NWs before deposition on a solid substrate (see Fig. 2-6e) [48-49].

(6) Contact transfer technique：The use of shearing force, tensile strength and other stress-contact methods, the one dimensional material contact printing on a substrate and have a arranged results (see Fig. 2-6f) [50-52].

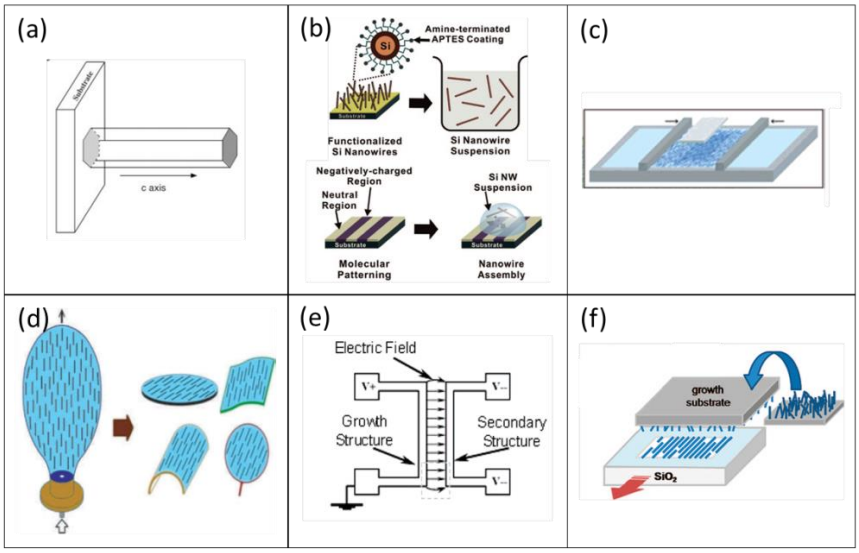

Fig. 2-6 Assembly methods for 1-D nanostructures (a) Flow-assisted alignment [41] (b) Deposition by chemical interactions [43] (c) Langmuir—Blodgett technique [45] (d) Blown-bubble technique [47] (e) Electric field directed deposition [49] (f) Contact transfer technique [51]

2.3 Hybrid Inorganic-Organic OTFTs

2.3.1 Introduction of hybrid TFTs

Conventional OTFTs are benefit from flexible and soluble molecular functionality, and large area process ability at low temperature, compatibility with plastics and cost down. Nevertheless, the inferior mobility and unstable in ambient constrain its applicability. Inorganic TFTs based high carrier mobility and well air stability, but also have some limitations. It can't have high mobility, flexibility, transparency and low-temperature manufacturing on one device. Unconventional hybrid materials combine many inorganic and organic materials favourable characteristics. It would be have great interest in electrical devices [53].

2.3.2 Material properties of organic semiconductor

One of the most important issues with regard to the development of high-performance polymer OTFTs is the high field-effect mobility. However, in

comparison with organic small molecule field-effect transistors, polymer OTFTs has a field-effect charge mobility lower by 1 to 2 orders of magnitude. Therefore, extensive efforts have been made for the improvement of the mobility in polymer OTFTs. In regioregular poly(3-hexylthiophene) (rr-P3HT) (see Fig. 2-7), the promising candidate for PFET, the mobility can be manipulated through polymer intrinsic properties (degree of regioregularity (RR) and molecular weight (Mn)) [54-56], and by introducing a self-assembled monolayer (SAM) onto the substrate surface [57]. To date, the highest mobility value among the rr-P3HT OTFTs ever documented is about 0.28 cm^2V^{-1} s^{-1} [58-59].

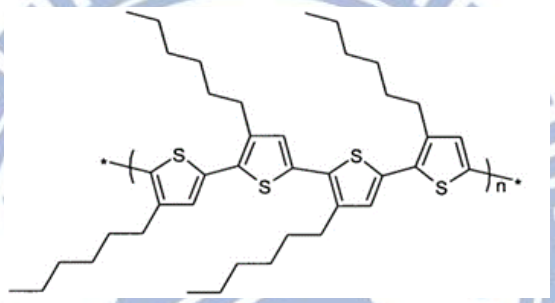

Fig. 2-7 Poly(3-hexylthiophene-2,5-diyl),P3HT structure [60]

2.3.3 Material properties of inorganic semiconductor

To the best of our knowledge, first Si wire growth was published by Treuting and Arnold in 1957 [61-62]. In the 1960s, Wagner and Ellis demonstrated vapor–liquid–solid (VLS) mechanism of single-crystal growth [63]. In this paper, they claimed their famous vapor–liquid–solid (VLS). For synthesize silicon wire, it's still a common way [64].

Si wire have good semiconducting properties. A different way to grow Si wire will also affect the characteristics. Relative to the organic semiconductor material Si wire have higher mobility and air stability [65-67].

2.4 Summary

For the OTFT, the active layer is the most important part of the functionality present on the transistor. In the active layer of the semiconductor material of their structure and properties are often decided the merits of the OTFT function. The experiment produced hybrid OTFT that is focused on the active layer carrier transport ability of the upgrade, as well as its air stability improvements.

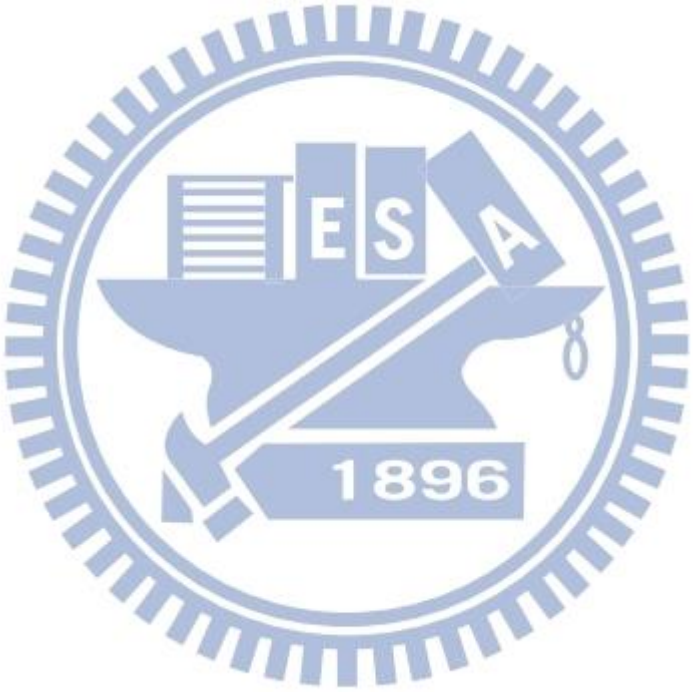

Chapter 3

Experimental Procedures

3.1 Fabrication Flow of Pristine Thin Film Transistors

The transistor structures employed in this study are bottom-gate-bottom-contact on a heavily doped n-type Si wafer with 200nm thermal oxide. For back gate contact, the backside SiO_2 layer was removed by RIE etching (OMNI-RIE, Duratek) with 180 s at 10 sccm of O_2 and 50 sccm of CF_4 for three cycles. The 200 nm measured by (J.A. Woollam Ellipsometer, Alpha-SE) of gate oxide SiO_2 layer (C_{ox} = 15 nF cm^{-2}, Agilent HP4145B semiconductor parameter analyzer with HP4140 quasi-static C-V instrument) was cleaned by acetone and iso-propyl alcohol (IPA). Standard photolithography (Table 3-1) was used to form a positive photoresist contacts on the gate oxide which have the source and drain pattern. Then, we use thermal metal evaporating to deposited source and drain metal layers. Cr is used as an adhesion layer, the electrodes is consisting of Cr/Au (5 nm/50 nm). Acetone was used to a standard lift-off process. It can remove the metal film on the top of the photoresist to form the metal film pattern. Cr/Au was used to be source/drain electrodes, then deposited of the organic semiconductor layer, the substrate were immersed in a solution of octyltrichlorosilane (OTS-8) (97%, Alfa Aesar) or n-octadecyltrichlorosilane (ODTS) (95%, contain 5-10% branched isomers, Alfa Aesar) in toluene (0.05 g mL^{-1}) at 60 ℃ for 20 min. After subsequent IPA rising, the surface-treated substrate were baked at 60 ℃ for 60 min. Finally the P3HT

polymer (18 mg mL^{-1}, 98.5% regional regular, 50,000 M.W., Uni Region Bio-Tech) was spin coated on the bottom-gate-bottom-contact transistor structure to form a thin film as the active layer. The coating and annealing process were carried out inside a N_2 glovebox (see Fig. 3-1).

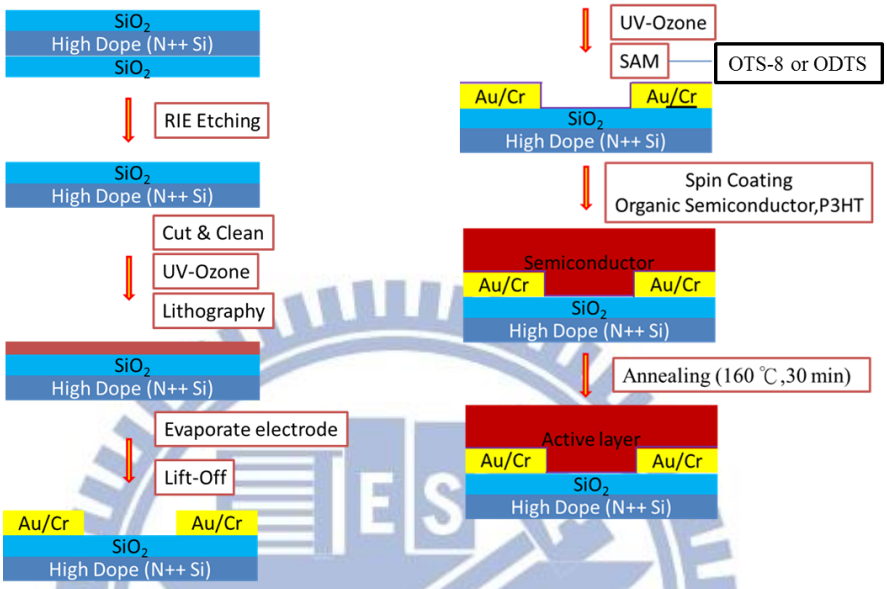

Fig. 3-1 Fabrication process of pristine OTFTs

Table 3-1 Standard photolithography parameters

Step	Process description	Parameters
1	Standard clean	sonication in acetone and IPA, 5 min , N_2 blow dry
2	Dehydration bake	120℃ hotplate, 1min, center of hotplate
3	HMDS coating	HMDS, 1000 rpm 15s then 3000 rpm 30s
4	HMDS baking	120℃ hotplate, 1min, center of hotplate
5	Coating PR	AZ5214E, 1000 rpm 15s then 3000 rpm 30s
6	Prebake PR	100℃ hotplate, 1min, center of hotplate
7	Mask alignment	Align mask with wafer, expose for 80 mJ cm^{-2}, G-line
8	Development	Use AD-10 developer, ~1 min, DI rinse 1min, N_2 blow dry
9	Inspection	Inspect for good transfer, exposure quality marks

3.2 Fabrication of Hybrid Thin Film Transistors

Preparation of Nanowires on PDMS film. Intrinsic Si NWs with diameters of ~10−60 nm and ~7 μm (see Fig. 3-2) in length were synthesized by chemical vapor deposition (provided by Dr. Ken Ogata, University of Cambridge) [68]. A polydimethyl-siloxane (PDMS) film (~0.7−1 mm thick, 20 mm in width, 40 mm in length) was formed by casting its prepolymer (Sylgard 184, Dow Corning), mixed with its curing agent at a ratio of 15:1 (w/w). NWs growth substrate contact transfer to 1cm×1cm Si wafer (surface treated with poly-L-lysine to increase the adhesion, Sigma-Aldrich) (yield: 50−60%). The PDMS film was placed on top of the Si wafer substrate, and after applying gentle manual pressure from the top, the film was quickly peeled to transfer the NWs to the PDMS surface (yield: 50−60%). While a single yield is not high, but the transfer can be repeated to increase yield [18].

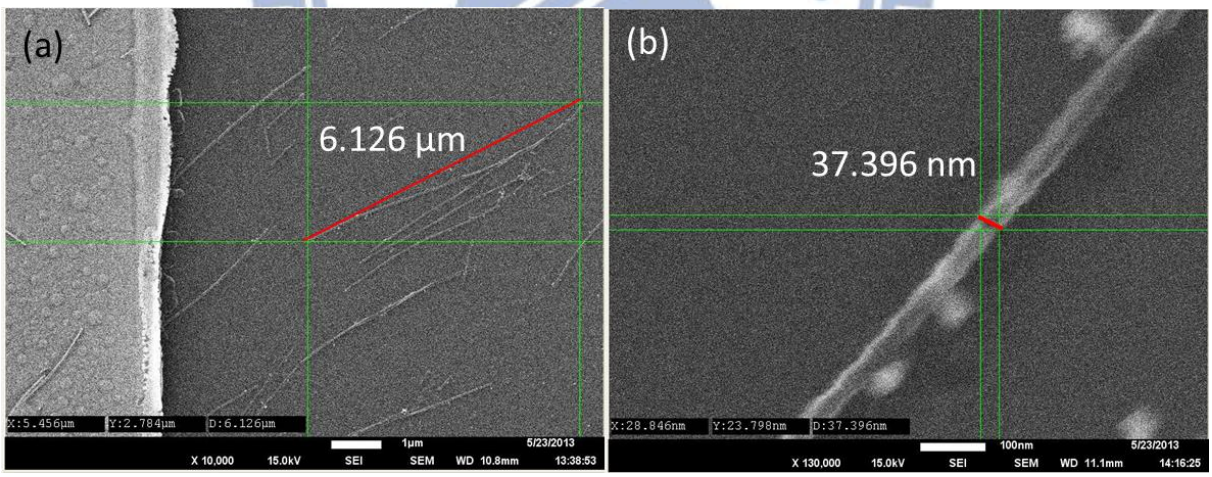

Fig. 3-2 SEM images of Si NWs. Scale bar : (a) 1μm and (b) 100 nm

Stretched Contact Printing for Assembling Nanowires. The controlled stretched contact printing was carried out using an home-built stretching machine (see Fig. 3-3). First, a PDMS each side fixed with a carrier that can be shifted along the length of a horizontal rail. The carrier can be moved slowly to

stretch the PDMS up to 100% of strain. The PDMS film with a random distribution of NWs was stretched to different distances at a controlled speed. Then, SiO_2 wafer was slowly moved down to transfer Si-NWs from the stretched PDMS film. NWs were transferred to the surface of a rigid Si/SiO_2 substrate (SiO_2 surface treated with poly-*L*-lysine to increase the adhesion) by stamping and then peeling back the PDMS at a relatively slow speed, forming a single layer of oriented NWs on the receiving substrate (see Fig. 3-4). Si-NWs in the flashlight irradiation appear blue reflective (see Fig. 3-5) [18].

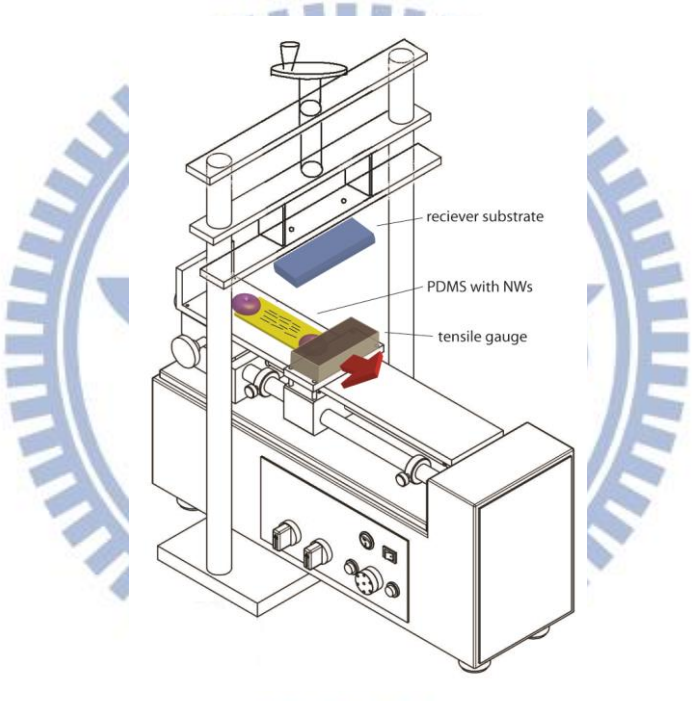

Fig. 3-3 Set-up of the home-built machine for stretched contact printing

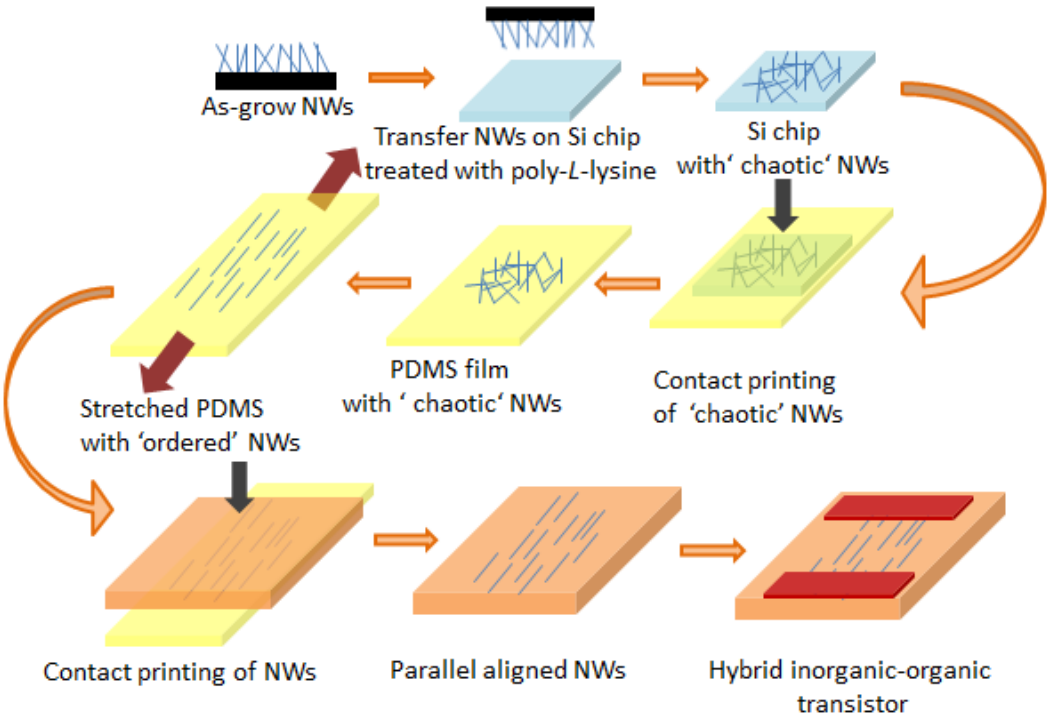

Fig. 3-4 Process flow of stretch contact printing

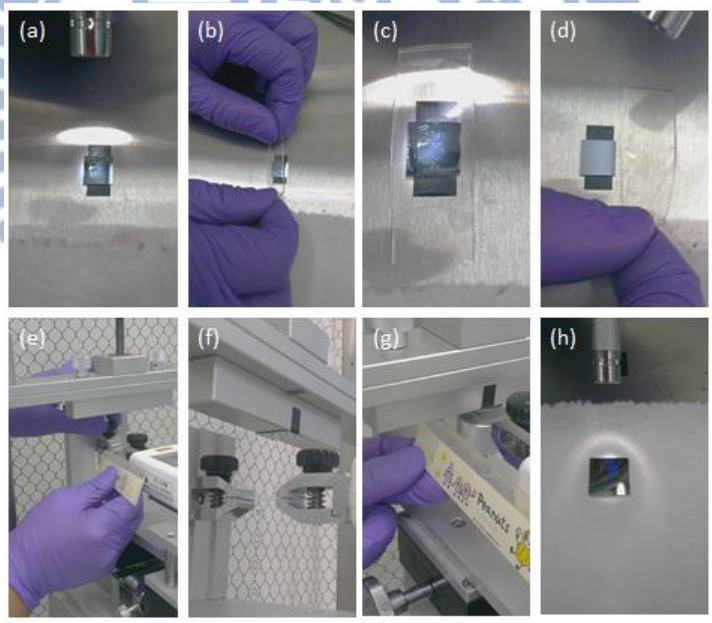

Fig. 3-5 Stretch contact printing operation (a) Transfer NWs on Si chip treated with poly-*L*-lysine (b)(c) Contact printing of ‘chaotic’ NWs (d) PDMS film with ‘chaotic’ NWs (e) PDMS fixed at stretcher and measure it’s length (f) SiO_2 Wafer fixed upon PDMS (g) Stretch PDMS for 100% of strain, then contact printing of NWs (h)Parallel aligned NWs on SiO_2 wafer

Hybrid Si-P3HT transistors fabrication. For hybrid TFTs, the Cr/Au (5 nm thick Cr, 50 nm thick Au) contacts were defined by conventional UV photolithography on the Si/SiO_2 substrates (200 nm thick SiO_2, C_{ox} = 15 nF cm^{-2}). with stretching-assembled Si NWs. Prior to self-assembled monolayer (SAM) surface treatment, the Si NW samples were dipped in a dilute HF (1:40) solution to remove their native oxide shells. An organic semiconductor poly(3-hexylthiophene-2,5-diyl), P3HT was spun-coat (at 500 rpm for 10 s and then 1200 rpm for 60 s) in a 1,2-dichlorobenzene solution (18 mg mL^{-1}) onto those substrates covered with Si NWs and Cr/Au electrodes. The coating process was carried out inside a N_2 glovebox. Pristine P3HT devices were also fabricated in the same manner without the stretched contact printing process. The devices were annealed at 160 ℃ in N_2 for 30 min (see Fig. 3-6) [18].

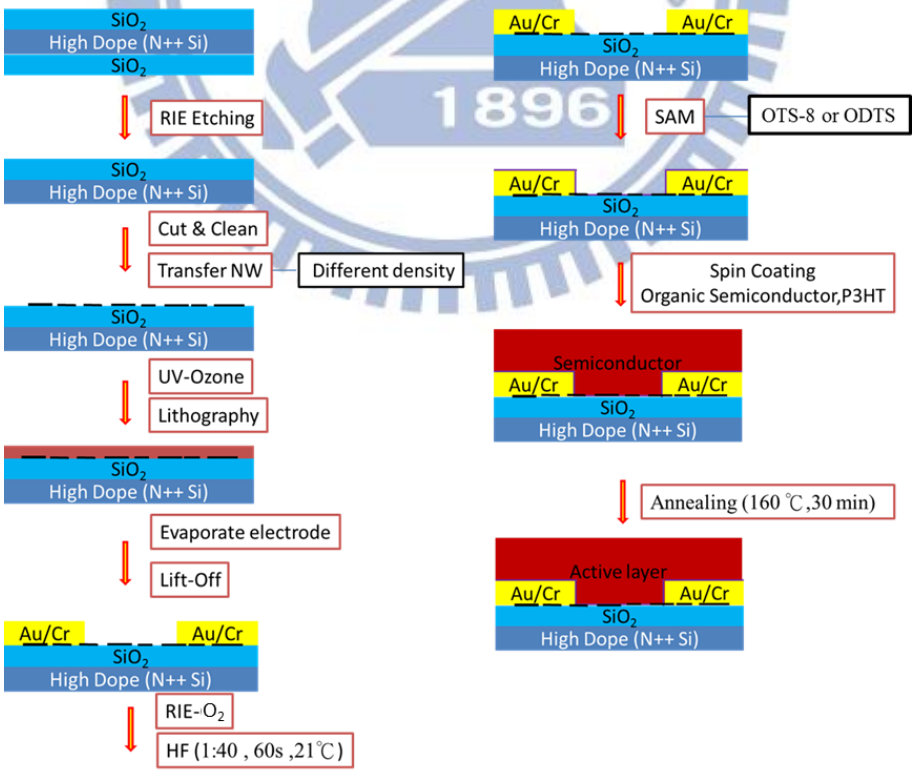

Fig. 3-6 Fabrication process of hybrid NW-P3HT TFTs

3.3 Electrical Measurement Methods

The devices electrical properties were measured by Agilent 4155C I-V analyzer in a light-isolated probe station at room temperature. In I_{DS}-V_{GS} measurement, the typical drain-to-source bias was swept from V_{GS} = -40 V to V_{GS} = 20 V. In I_{DS}-V_{DS} measurement, the typical drain-to-source bias was swept from V_{DS} = 0 V to V_{DS} = -40 V.

In this section, it describe the methods of typical parameters extraction such as threshold voltage (V_T), subthreshold swing (SS), ON/OFF current ratio (I_{ON}/I_{OFF}) and field effect mobility (μ_{FE}) from device characteristics.

3.3.1 Determination of the V_T

Threshold voltage (V_T) was defined from the gate to source voltage at which carrier conduction happens in OTFT channel. V_T is related to the gate insulator thickness and the flat band voltage. Plenty of methods are available to determine V_T which is one of the most important parameters of semiconductor devices. In this thesis, I_{DS} take the square root of the number, and take a linear approximation way to get V_T (see Fig 3-7).

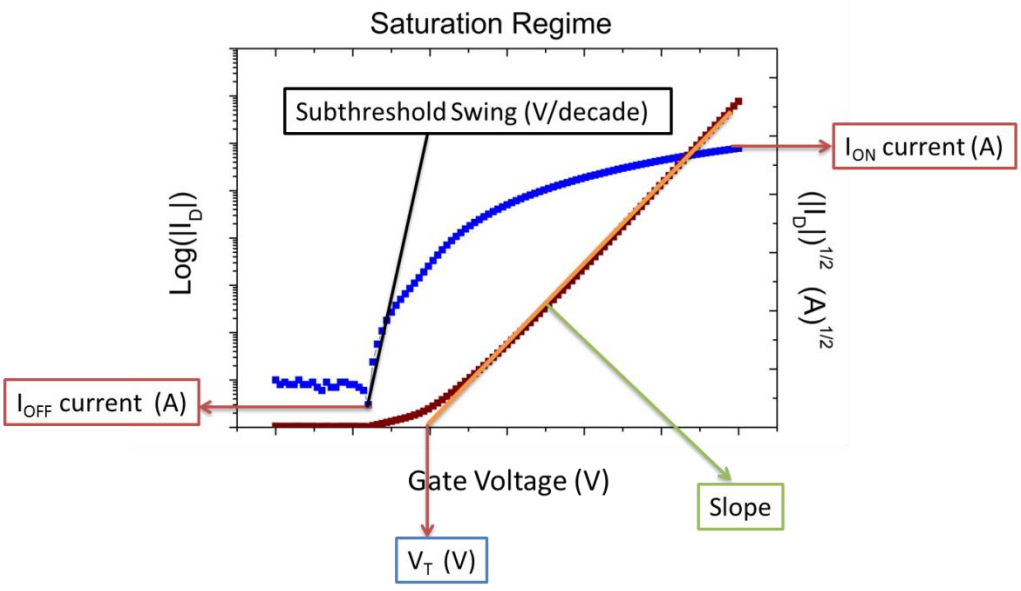

Fig. 3-7 Parameter extraction method in the thesis

3.3.2 Determination of the Subthreshold Swing

Subthreshold swing (S.S., V decade^{-1}) is a typical parameter to describe the control ability of gate toward channel which is the speed of turning the device on and off. In this study, S.S. was defined as the gate voltage required to decrease the threshold current by two orders of magnitude (from 10^{-10}A to 10^{-8}A). The threshold current was specified to be the drain current when the gate voltage is equal to $V_{T.}$

3.3.3 Determination of the field effect mobility

Typically, by I_{DS}-V_{GS} curve, we calculated with the formula 3-1 which can be obtained field-effect mobility (μ_{FE}) and threshold voltage (V_T) at high negative drain bias (V_{DS} = -40 V), $V_{SD} \geq (V_{SG}–V_T)$. The OTFT transfer I-V characteristics can be expressed in saturation region as

$$I_{SD} = \mu_{FE} C_{OX} \frac{W}{2L}(V_{SG}-V_T)^2 \quad \text{(3-1)}$$

Where

C_{OX} is the gate oxide capacitance per unit area,

W is channel width, L is channel length,

V_T is the threshold voltage.

Square root of the formula 3-1 can be obtained, and the conversion formula 3-1 as formula 3-2.

$$I_{SD}^{1/2} = \sqrt{\frac{W\mu_{FE}C_{OX}}{2L}}\ (V_{SG}-V_T) \quad \text{(3-2)}$$

The formula 1-3 as the slope formula $y = a(x-\frac{b}{a})$; $y = I_{SD}^{1/2}$; $x = V_{SG}$, we can get

$a=\sqrt{\frac{W\mu_{FE}C_{OX}}{2L}}$, then $\mu_{FE} = a^2 \frac{2L}{WC_{OX}}$, $V_T = \frac{b}{a}$

The transconductance is defined as

$$g_m = \mu_{FE} C_{OX} \frac{W}{L} V_{SD} \quad \text{(3-3)}$$

Thus,

$$\mu_{FE} = \frac{L}{W C_{OX} V_{SD}} g_m \quad \text{(3-4)}$$

Similarly, that can get mobility in the saturation region as

$$\mu_{FE} = \frac{2L}{W C_{OX}} \left(\frac{\partial \sqrt{I_{SD}}}{\partial V_{SG}}\right)^2 \quad \text{(3-5)}$$

If V_{SD} is much smaller than $V_{SG} - V_T$, i.e. $V_{SD} << (V_{SG} + V_T)$ and $V_{SG} > -V_T$, the drain current can be approximated in linear region as

$$I_{SD} = \mu_{FE} C_{OX} \frac{W}{L} [(V_{SG} - V_T) V_{SD} - \frac{1}{2} V_{SD}^2] \quad \text{(3-6)}$$

3.3.4 Determination of ON/OFF Current Ratio

ON/OFF current ratio is another important factor of OTFTs. High ON/OFF current ratio represents not only the large turn-on current but also the small off current (leakage current). It affects display gray levels (the bright to dark state number) directly. There are many methods to specify the on and off current. The easiest one is to define the maximum current as on current and the minimum leakage current as off current while drain voltage equal to -40 V.

$$\textit{ON/OFF ratio} = \frac{I_{DS,MAX}}{I_{DS,MIN}} \quad \text{when } V_{DS} = -40 \text{ V} \quad \text{(3-7)}$$

Chapter 4

Results and Discussion

This chapter content two parts : pristine P3HT TFTs and hybrid TFTs. The characteristics of pristine P3HT is evaluated based on different fabrication conditions. With the optimized conditions of P3HT, the hybrid TFTs with polythiophene -nanowires semiconducting layer are investigated loading effect of aligned NWs on transistor performance is discussed and relative problems observed are also addressed. Atomic force microscope (AFM), scanning electron microscope (SEM), and X-ray diffraction (XRD) were used to analyze the surface properties of thin film and NWs. Discussion and analysis framework can be seen in Fig. 4-1.

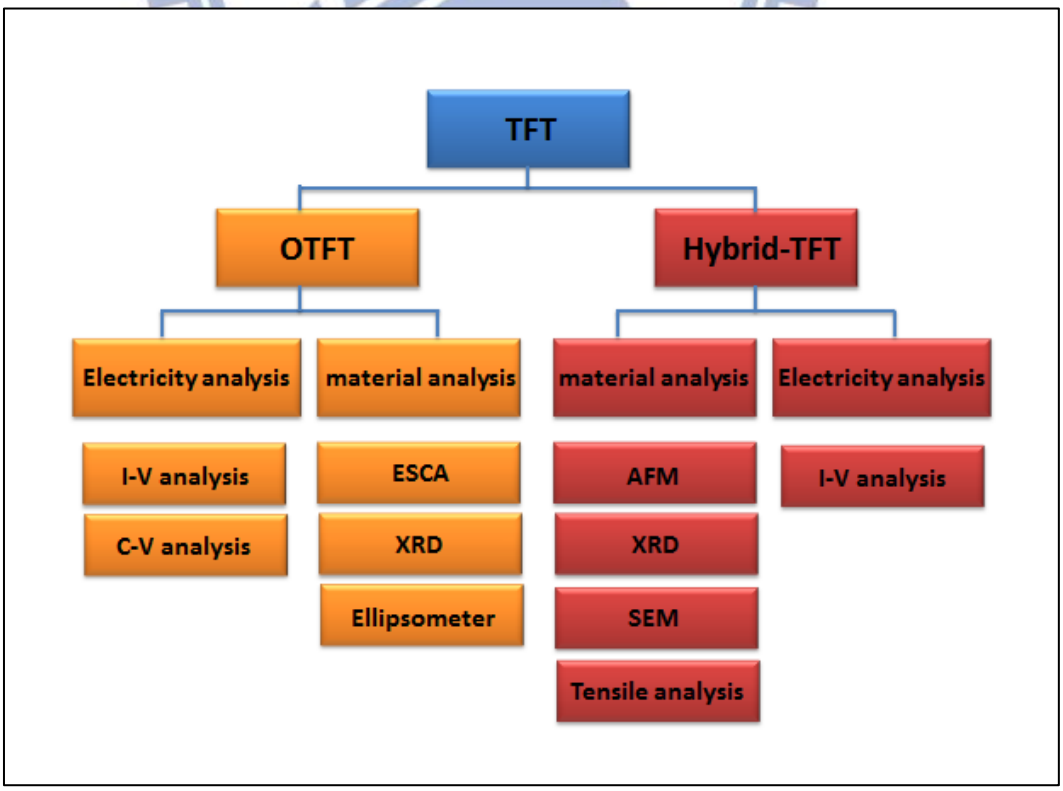

Fig. 4-1 Discussion and analysis framework in this thesis

4.1 HF dipping effect on P3HT transistors

After comparison Pristine P3HT device and hybrid OTFT (NW=0, HF-P3HT), Fig. 4-2 and Table 4-1 show after HF treatment mobility is higher, I_{ON} and I_{OFF} is higher, ON/OFF ratio is lower, V_T is larger. But, both in mobility, ON / OFF ratio and V_T just have a little difference. Therefore, that HF process does not affect the characteristics of P3HT OTFT too much. Then, use AFM to measure the SiO_2 roughness before and after HF treatment. Image Rmax shows after HF treatment, the surface roughness is 4.72 nm higher than SiO_2 2.72 nm (see Fig. 4-3). V_T associated with several factors: The interface charge trap density on the insulating layer, the source and drain contact quality and the internal existed conducting channel [69]. After HF treatment will also affect the V_T. The V_T of Pristine P3HT is closer to zero. It has a lower operating voltage.

Image Rmax : Maximum vertical distance between the highest and lowest data points in the image [70].

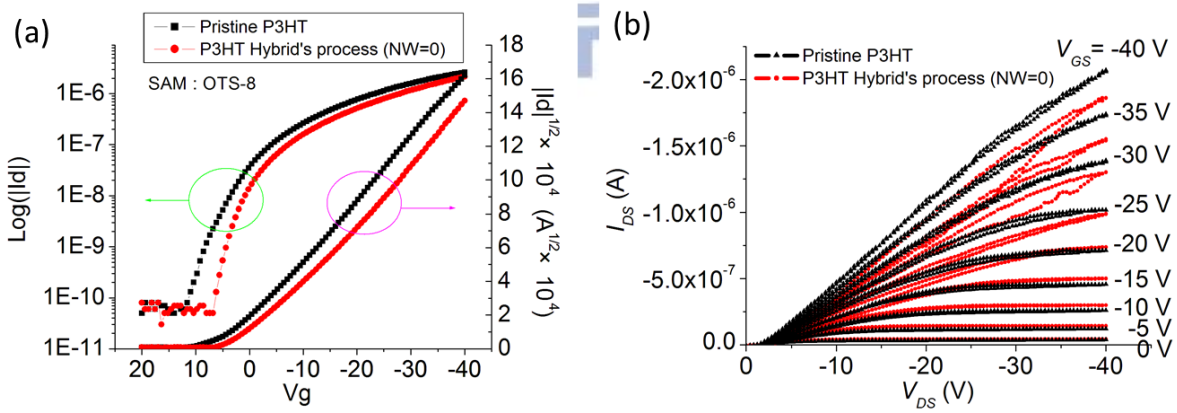

Fig. 4-2 Electrical performance of Pristine P3HT device and hybrid OTFT (NW=0)

Table 4-1 Comparison of the relative parameters for Pristine P3HT device and hybrid OTFT (NW=0)

	Mobility ($cm^2V^1S^{-1}$)	I_{ON} (A)	I_{OFF} (A)	ON/OFF ratio	V_T (V)
Pristine P3HT	0.007	2.16×10^{-6}	3.00×10^{-11}	7.20×10^{4}	0.25
P3HT Hybrid's process (NW=0)	0.008	2.63×10^{-6}	5.00×10^{-11}	5.26×10^{4}	3.42

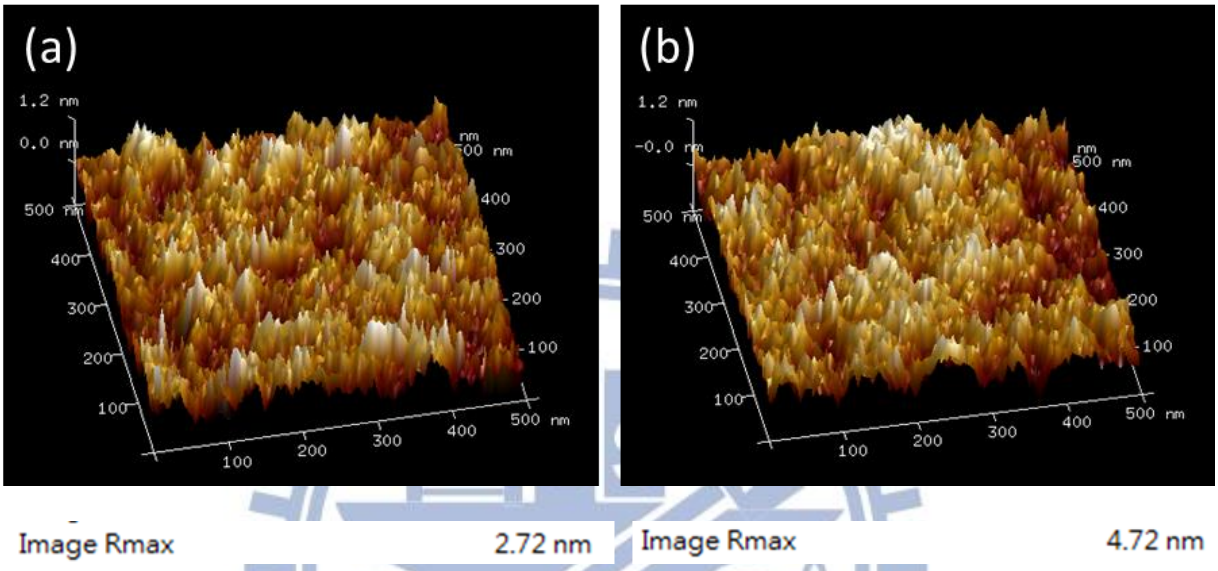

Fig. 4-3 AFM 3D view of (a) SiO_2 (b) SiO_2 by HF treatment

4.2 SAM effect on P3HT TFTs

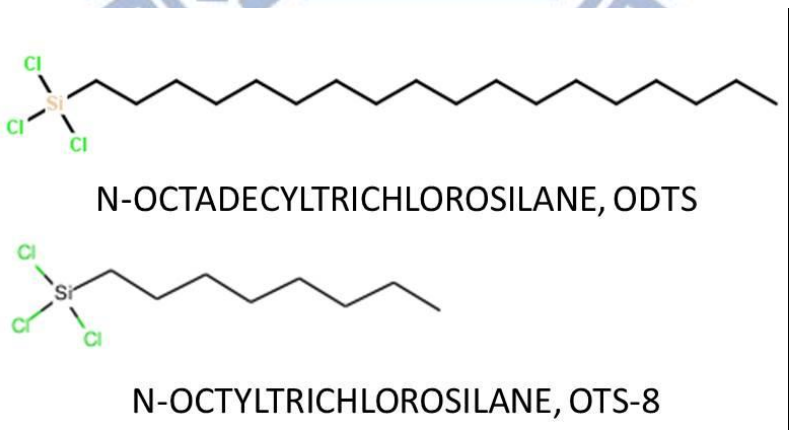

Fig.4-4 ODTS and OTS-8 molecule structure [71-72]

Because has been reported that longer alkyl chain ODTS more than OTS-8 (see in Fig.4-4) improve the characteristics of a semiconductor arrangement, we compared the effect of two SAM [73]. Although HF treatment increased surface

roughness and defects, cause an irregular curve. ODTS I_{DS}-V_{DS} curve is smoother, and saturated zone moves to the left (see Fig. 4-5). It can be seen through the ODTS treatment have been better surface modification effect on OTFTs. In this thesis, experimental results also indicate that, ODTS in enhancing OTFT carrier mobility is relatively higher than OTS-8 under the same process. ODTS mobility is 1.37 times of OTS-8, ON/OFF ratio is in the same order. According to the section 4.1 of the reasons mentioned affect V_T. The type of surface treatment can also impact the V_T (See Table 4-2). After the transfer nanowire surface roughness caused increases, ODTS has a better effect than OTS-8 in the modified surface.

XRD(glancing incident angle diffraction, ATX-E & D/MAX2500, Rigaku) figure shows that P3HT has higher crystallinity after SAM treatment (see Fig. 4-6a). Compare to OTS-8 and ODTS, we found ODTS is better (see Fig. 4-6b).

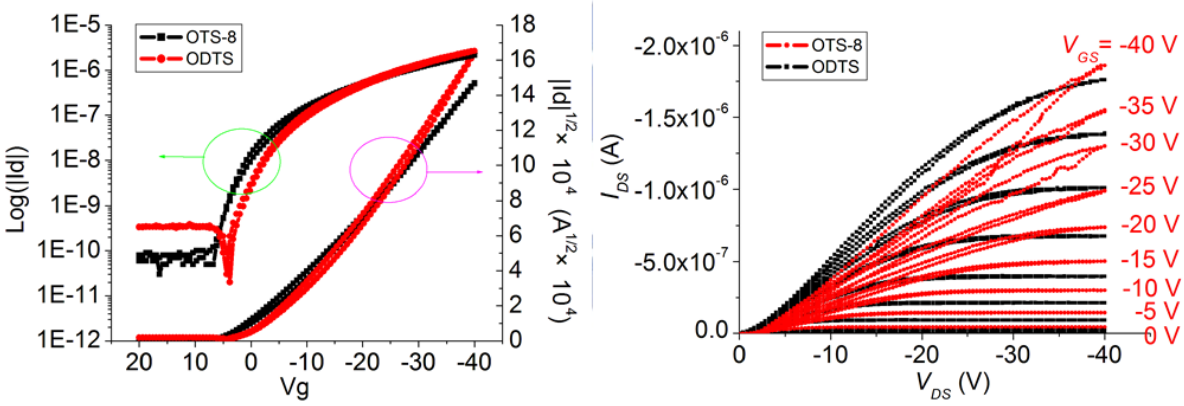

Fig. 4-5 Electrical performance of OTS-8 device and ODTS on hybrid OTFT

Table 4-2 Comparison of the relative parameters for OTS-8 device and ODTS on hybrid OTFT

	Mobility ($cm^2V^1S^{-1}$)	I_{ON} (A)	I_{OFF} (A)	ON/OFF ratio	V_T (V)
ODTS	0.010	2.69×10^{-6}	3.00×10^{-11}	8.97×10^{4}	-3.20
OTS-8	0.008	2.63×10^{-6}	5.00×10^{-11}	5.26×10^{4}	3.42

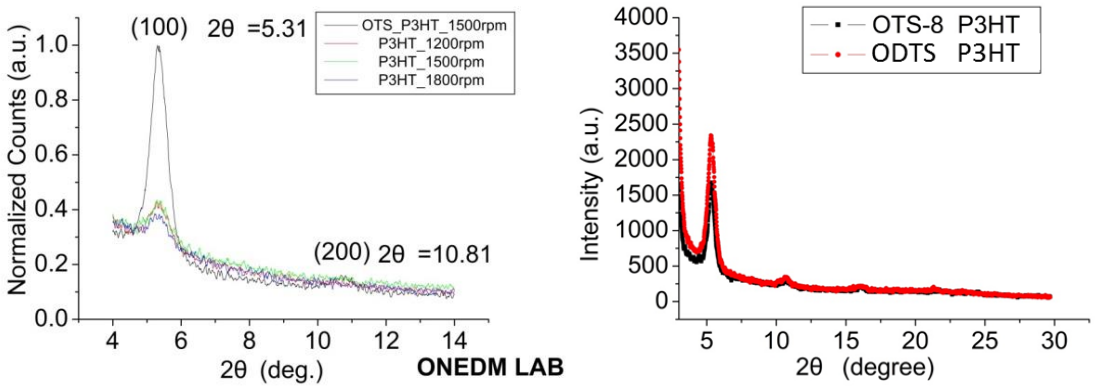

Fig. 4-6 (a) P3HT film XRD with and without SAM treatment (b) P3HT film XRD with OTS-8 and ODTS

4.3 Stretched Contact printing for NW assembly

In this study, recently published stretching imprinting method was used to test the tensile properties of PDMS, in order to understand the arrangement of nanowires by stretched data. PDMS in the elastic range is proportional to the force and elongation (see Fig. 4-7). This work produced the maximum elongation of the PDMS can be three times the original length. PDMS will be found in elastic fatigue when elongation more than doubled. Elongation of PDMS is on many factors, such as concentration, thickness, width and length.

The experimental results of NWs assembling are shown in Fig. 4-8. Our home-built stretching machine for stretched contact printing can provide a reliable control, transforming a random distributed network (see Fig. 4-8a) into a highly oriented layout (see Fig. 4-8b). A large-area of parallel aligned NWs can be achieved and then proceeded with the source-drain electrodes (see Fig. 4-8c, d) for TFT fabrication.

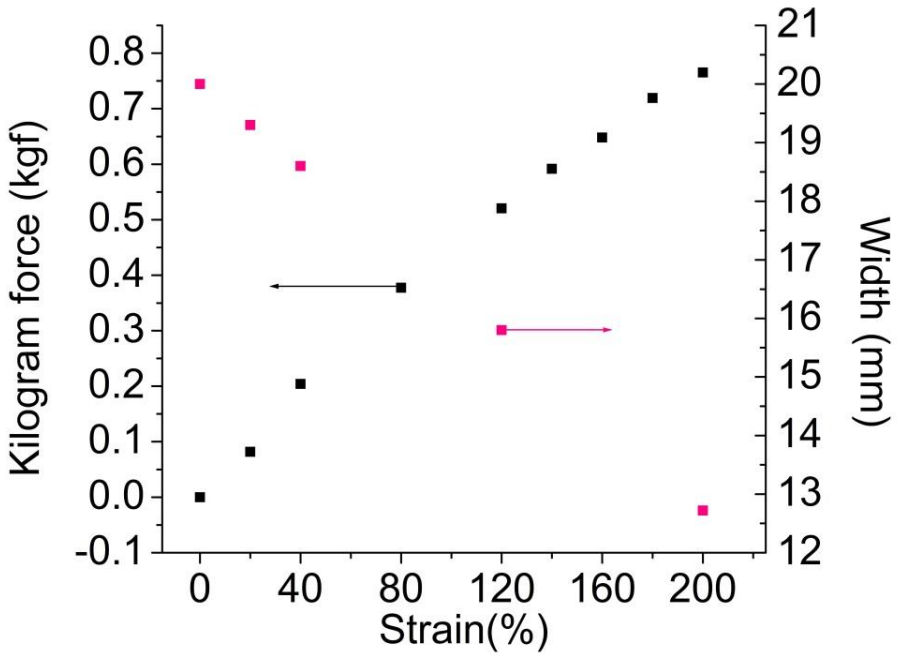

Fig. 4-7 PDMS tensile test results

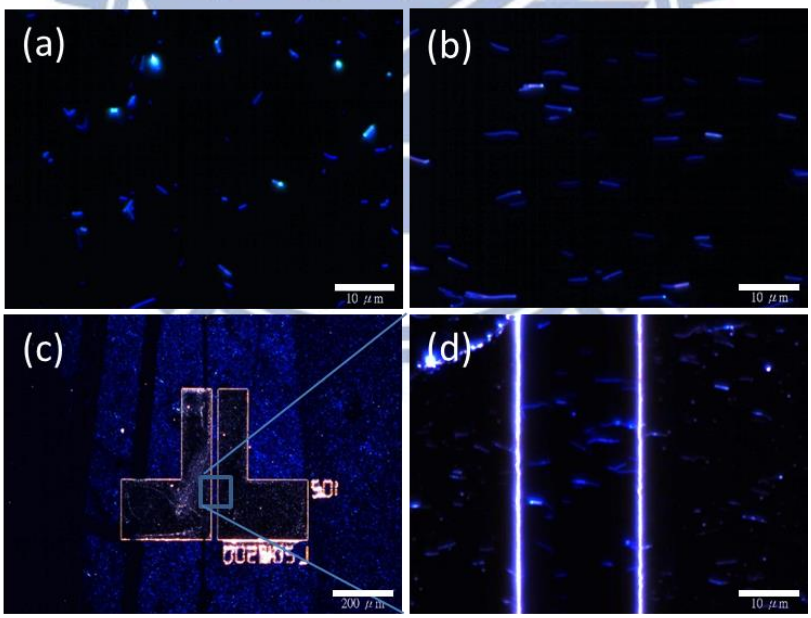

Fig. 4-8 Dark field optical microscope images of (a) random distributed NW arrays, (b) parallel aligned NWs array after stretched contact printing process (scale bar: 10um), (c) large-area aligned NWs covered with contacted electrodes (scale bar: 200um), and (d) NWs array in the active channel (scale bar: 10 μm)

4.4 SEM and AFM Result of NWs-P3HT

From the SEM (FE-SEM 7001, JEOL) photographs of view, because some NWs diameter is not the same and not fully attached to the SiO_2 surface, resulting NWs piercing appear on the electrode metal film phenomenon (see Fig. 4-8a). This also means that the NWs in the channel will also exhibit this phenomenon. NWs not attached to the SiO_2 will cause holes. It causes hybrid OTFT carrier transitivity damaged. If this phenomenon can be improved, I believe that the carrier transitivity will have a positive impact. From the AFM images, due to the size of nanowire radius is not consistent, after the HF etching negative SiO_2 of NWs, it will drift away from the surface or reattached. It causes portion consistency reduces of NWs orientation. NWs attached SiO_2 incomplete and curling phenomenon that may affect the carriers transport. The Irregularities and defects of electrode will also limit the carrier transport (see Fig. 4-9b).

In the case of NWs density was low, AFM (Tapping mode, Innova, Bruker) image shows that aligned NWs were embedded without interrupting polycrystalline P3HT domains (grain size ~100 nm) (see Fig. 4-10). Which will make transfer of P3HT carrier is not affected, and can effectively deliver carrier to NWs.

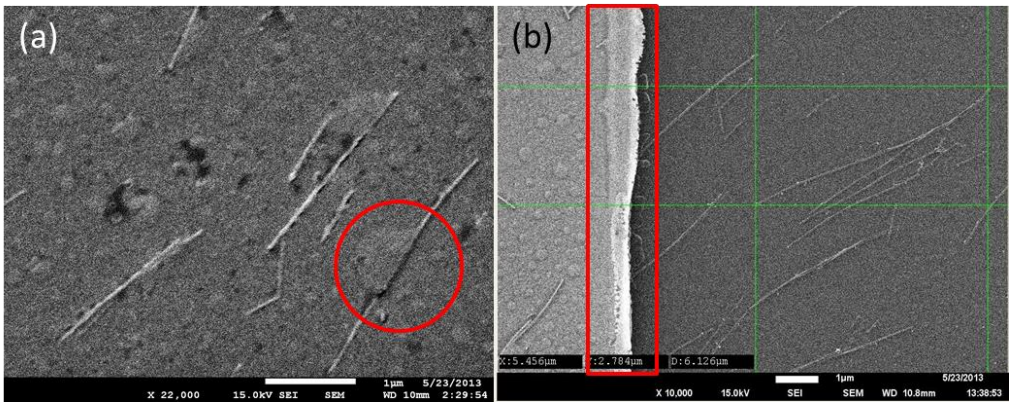

Fig. 4-9 The SEM results of (a) NWs on electrode (b) interface between

electrode and channel

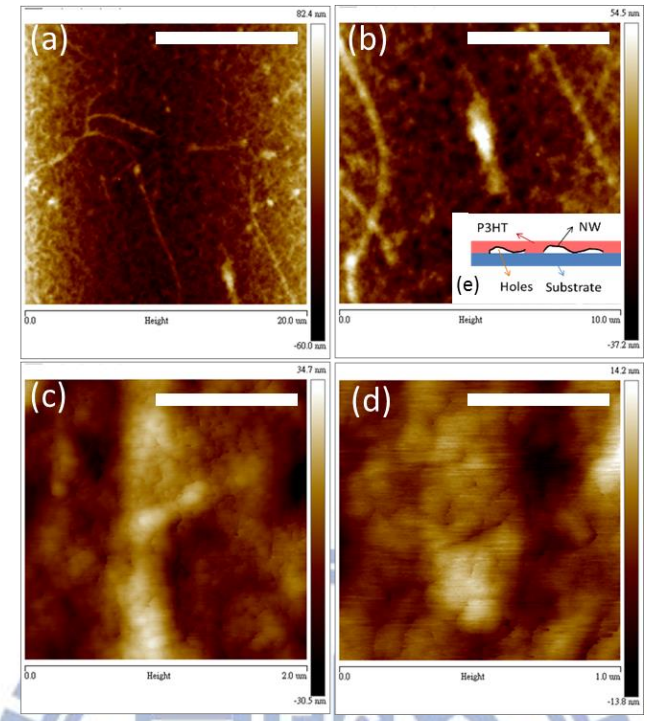

Fig. 4-10 The AFM results of NWs embedded in channel. Scale bar (a)10μm (b)5μm (c)1μm (d)500 nm (e) schematic of NWs curling

4.5 The Results of Hybrid OTFTs

The electrical measurement results of the fabricated hybrid Si-P3HT TFTs with the different NWs loading in the active channel are presented in Table. 4-3. Fig. 4-11a shows the device mobility and on/off ratio are proportional to the NW loading. Fig. 4-11b shows that with the NWs increased make maximum output current curve continued upward. Fig. 4-11c, d show saturation curve more obvious in NW=0. I_{DS}-V_{DS} curve will also be affected with the NWs increased. Fig. 4-11e, f show device performance data measured periodically over 600 hours after fabrication. Our hybrid transistors were relatively stable in ambient conditions (exposed to air, moisture, and stored in dark). It is found after transistor reduced mobility and ON / OFF ratio cause exposed to air , through heated device for 5 min at 180 ℃ (in ambient), the electrical properties will be

recovered. This also proves that transistor is indeed decreased electrical performance caused by oxygen and moisture adsorption. It can be assuming the moisture play an important role than oxygen. Because the temperature if not heated above 100 ℃, then the effect is not significant response, and we know the boiling point of water at 100 ℃. The key mechanism might be charge carriers transport through these Si-NWs as a speedy path in the active channel to increase the field effect mobility in the hybrid devices. However, remove the native oxide shells surrounded the Si NWs is very crucial process prior to P3HT deposition. In our situation, the HF etching process is highly affected by solution temperature, which make difficult to control the etching rate. Moreover, there is no clear influence on the status of crystalling P3HT from current NW loading density (see Fig. 4-12).

Note that the interaction affecting charge transport between Si NWs and thiophene molecules we have yet to understand clearly. This t

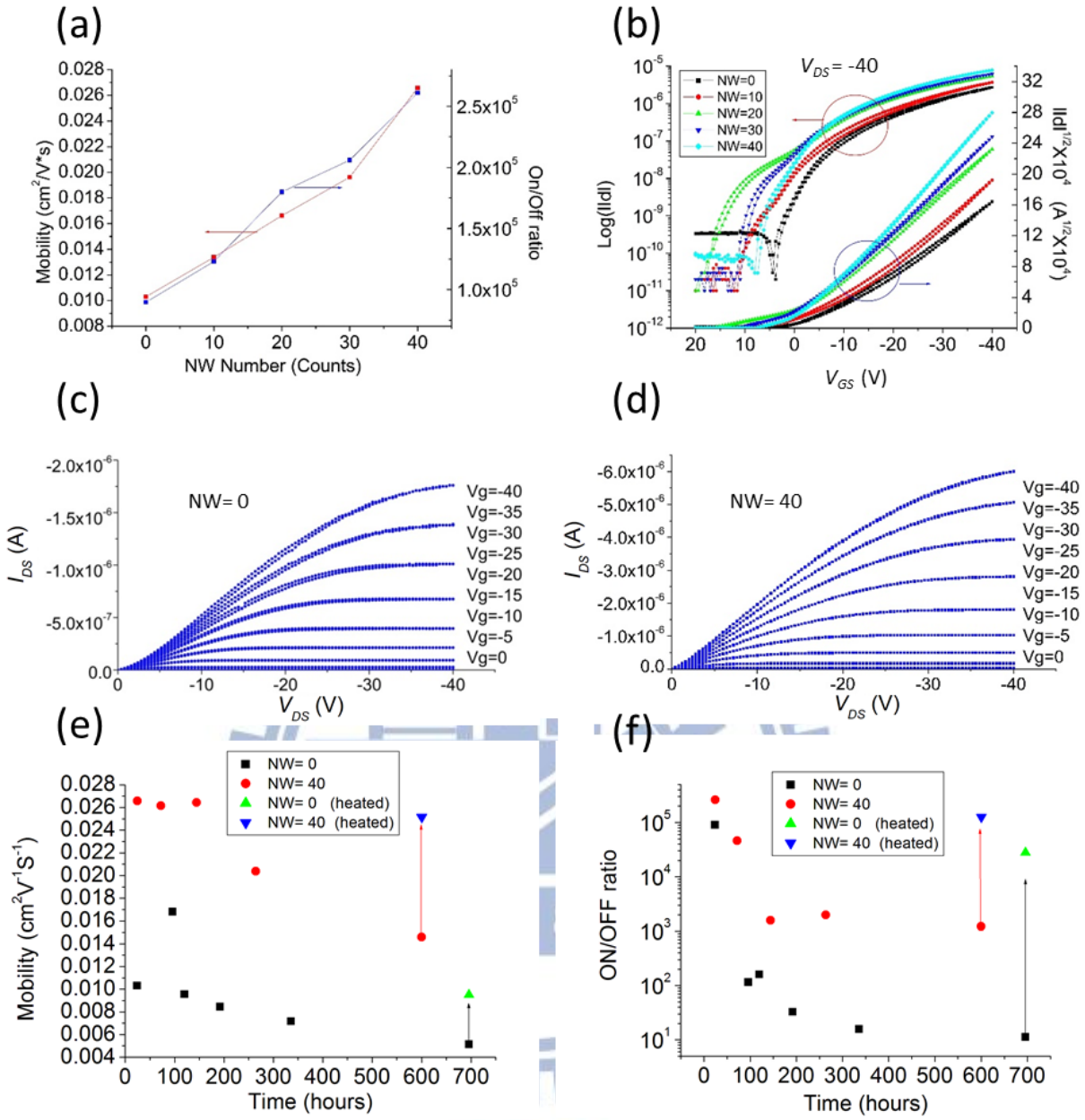

Fig. 4-11 (a) NWs loading effect on mobility and on/off ratio of the hybrid Si-P3HT transistors (b) Transfer characteristics from the hybrid devices with different NWs loading at V_{DS} = -40V. Output characteristics of (c) a P3HT transistor and (d) a Si-P3HT device with a loading of 40 NWs. Air stability test on (e) mobility and (f) ON/OFF ratio from a P3HT and a Si-P3HT TFTs.

Table 4-3 Comparison of the relative parameters for Different Si-NWs density in hybrid OTFT

NW	Mobility ($cm^2V^{-1}S^{-1}$)	I_{ON} (A)	I_{OFF} (A)	ON/OFF ratio	V_T (V)	SS ($V\ dec^{-1}$)
0	0.010	-2.69×10^{-6}	-3.00×10^{-11}	8.97×10^{4}	-3.2	2.81
10	0.013	-3.70×10^{-6}	-3.00×10^{-11}	1.23×10^{5}	-2.48	4.21
20	0.017	-5.40×10^{-6}	-3.00×10^{-11}	1.80×10^{5}	1.76	1.89
30	0.020	-6.17×10^{-6}	-3.00×10^{-11}	2.06×10^{5}	0.916	1.83
40	0.027	-7.83×10^{-6}	-3.00×10^{-11}	2.61×10^{5}	-0.423	2.56

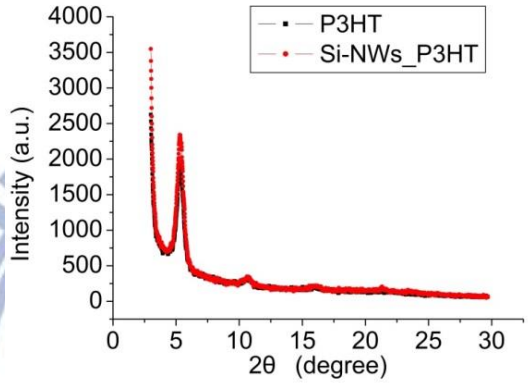

Fig. 4-12 Comparison P3HT film XRD curve with and without NWs

4.6 Summary

After discussion and analysis of the experimental data, it can be integrated the following results : (1) After SAM processing, P3HT get a better crystallinity, and can effectively improve transport properties of semiconductor. (2) To be a SAM, ODTS is better than OTS-8 in SiO_2 treatment for P3HT crystallinity. (3) After loaded NWs in channel, it can effectively enhance the semiconductor properties, especially on the mobility and stability in this thesis. (4) Heated to remove water and oxygen might be a one way to recover the semiconductor conducting characteristics.

Chapter 5

Conclusions

5.1 Conclusion

In this study, first discussion is how to optimize the characteristics of pristine P3HT OTFT. It achieved good results, when using the SAM, OTDS. In the production of hybrid OTFT, we need to have such a stabilization technology. This thesis also discusses the tensile properties of PDMS. Because this study need it to further understand stretched contact printing technology in application of stretch PDMS to align one dimensional materials.

After above work, this thesis fabricated hybrid-based TFTs with a nanocomposite conducting channel of a parallel aligned nanowire network and an organic polymer. With the incorporation of a small amount of semiconducitng nanostructures, an enhancement on device on/off ratio, mobility and air stability is achieved from those hybrid networks. From the AFM and XRD analysis, Si NWs did not affect the P3HT crystallization and also have positive effect on the electrical property. Furthermore this thesis also found that re-annealed can help the reduced electrical properties of transistors recovery. It will be very appealing if a higher density network of nanowire can be generated for these hybrid systems. More interaction of one dimensional materials and organic semiconductors will be studied. A variety of one dimensional composite material will continue to play an important role in the TFTs.

5.2 Future work

This experiment produced hybrid TFTs still have many places to improve and research. We will discuss the case of higher density of one dimensional materials and the interaction with organic semiconductors. To achieve this purpose, develop new technology to produce higher density of one dimensional material is required. The interaction between one dimensional materials and organic semiconductor is not yet fully understood. We hope to be able to use other ways to understand the charge carrier transport mechanism for one dimensional material in the hybrid TFT, such as kelvin probe force microscope. Using different organic-inorganic composite material can help us to understand the hybrid OTFTs property. I hope we can make hybrid TFTs with better electrical properties and applied on flexible substrates in the future.

Reference

[1] J. E. Lilienfeld, "Method and Apparatus for Controlling Electric Currents," U. S. Patents, 1745175, 1930.

[2] J. Bardeen, W. H. Brattain, “The Transistor, a Semiconductor Triode”, Physical Review Letters, vol. 74, pp. 230, 1948.

[3] D. Kahng, M. M. Atalla, "Silicon-Silicon Dioxide Field Induced Surface Devices," Solid State Res. Conf., Pittsburgh, USA, 1960.

[4] H. Shirakawa, E. J. Louis, A. G. Macdiarmid,C. K. Chiang, and A. J. Heegerh, "Synthesis of Electrically Conducting Organic Polymers: Halogen Derivatives of Polyacetylene, (CH)x," Journal of the Chemical Society, Chemical Communications, pp. 578-580, 1977.

[5] Koezuka, A. Tsumura, T. Ando, "Field-Effect Transistor with Polythiophene Thin Film," Synthetic Metals, vol. 18, pp. 699–704, 1987.

[6] J. Takeya, M. Yamagishi, Y. Tominari, R. Hirahara, Y. Nakazawa, T. Nishikawa, T. Kawase, T. Shimoda, S. Ogawa, "Very High-Mobility Organic Single-Crystal Transistors with In-Crystal Conduction Channel," Applied Physics Letters, vol. 90, pp. 102120, 2007.

[7] A. L. Briseno, S. C. B. Mannsfeld, M. M. Ling, S. Liu1, R. J. Tseng, C. Reese, M. E. Roberts, Y. Yang, F. Wudl, Z. Bao, "Patterning organic single-crystal transistor arrays," Nature, vol. 444, pp. 913−917, 2006.

[8] N. A. Minder, S. Ono, Z. Chen, A. Facchetti, A. F. Morpurgo, "Band-Like electron transport in organic transistors and implication of the molecular structure for performance optimization," Advanced Materials, vol. 24, pp. 503–508, 2012.

[9] O. D. Jurchescu, J. Baas, and T. T. M. Palstra, "Effect of Impurities on the Mobility of Single Crystal Pentacene," Applied Physics Letters, vol. 84, pp. 3061–3063, 2004.

[10] H. Klauk, "Organic thin-film transistors," Chemical Society Reviews, vol. 39, pp. 2643-2466, 2010.

[11] RDECOM, "Flexible Plastic Display," www.flickr.com/photos/rdecom/

[12] K. Kuribara, H. Wang, N. Uchiyama, K. Fukuda, T. Yokota, U. Zschieschang, C. Jaye, D. Fischer, H. Klauk, T. Yamamoto, K. Takimiya, M. Ikeda, H. Kuwabara, T. Sekitani, Y. L. Loo, T. Someya "Organic Transistors with High Thermal Stability for Medical Applications," Nature Communications, vol. 3, 723,2012.

[13] H. Sirringhaus, T. Kawase, R. H. Friend, T. Shimoda, M. Inbasekaran, W. Wu, E. P. Woo, "High-Resolution Inkjet Printing of All-Polymer Transistor Circuits," Science, vol. 290, pp. 2123-2126, 2000.

[14] S. R. Forrest, "The Path to Ubiquitous and Low-Cost Organic Electronic Appliances on Plastic," Nature, vol. 428, pp. 911-918, 2004.

[15] R. R. Navan, B. Panigrahy, M. S. Baghini, D. Bahadur, V. R. Rao, " Mobility Enhancement of Solution-Processed Poly(3-Hexylthiophene) Based Organic Transistor Using Zinc Oxide Nanostructures," Composites Part B, vol. 43, pp. 1645-1648, 2012.

[16] G. W. Hsieh, J. Wang, K. Ogata, J. Robertson, S. Hofmann, W. I. Milne, "Stretched Contact Printing of One-Dimensional Nanostructures for Hybrid Inorganic−Organic Field Effect Transistors," Journal of Physical Chemistry C, vol. 116, pp. 7118-7125, 2012.

[17] T. Takenobu, N. Miura, S. Y. Lu, H. Okimoto, T. Asano, M. Shiraishi and Y. Iwasa, "Ink-Jet Printing of Carbon Nanotube Thin-Film Transistors on Flexible Plastic Substrates," Applied Physics Express vol 2, 2009, pp.0250051-0250053.

[18] K.Y. Cheng, G. W. Hsieh, "Hybrid Thin-Film Transistors Based on Nanocomposite P3HT and Silicon Nanowire Networks," Optics and Photonics Taiwan, International Conference 2013.

[19] Z. Bao, "Self-Assembly in Organic Thin Film Transistors for Flexible Electronic Devices," Material Matters, vol. 1, pp. 11-14, 2006.

[20] AIST, "n-Type Organic Thin Film Transistor Prepared by Printing Method," http://www.aist.go.jp, 2013.

[21] S. Stafstrom, "Electron Localization and the Transition from Adiabatic to Nonadiabatic Charge Transport in Organic Conductors," Chemical Society Reviews, vol. 39, pp. 2484–2499, 2010.

[22] Nabok, Alexei, "Organic and Inorganic Nanostructures (2 ed.)," Artech House Publishers, 2005.

[23] R. A. Marcus, "Electron-Transfer Reactions in Chemistry-Theory and Experiment," Reviews of Modern Physics, vol. 65, pp. 599-610, 1993.

[24] "Organic Semiconductor : Charge Transport in Disordered Organic Semiconductors," en.wikipedia.org/wiki/Organic_semiconductor

[25] Stanford Synchrotron Radiation Lightsource, "Highly Oriented Crystals in Polythiophenes,'' Science Highlight, 2006.

[26] S. Obata, Y. Shimoi, "Control of Molecular Orientations of Poly(3-hexylthiophene) on Self-Assembled Monolayers: Molecular

Dynamics Simulations," Physical Chemistry Chemical Physics, vol. 15, 9265, 2013.

[27] W. H. Lee, J. H. Cho, K. Cho, "Control of Mesoscale and Nanoscale Ordering of Organic Semiconductors at the Gate Dielectric/Semiconductor Interface for Organic Transistors," Journal of Materials Chemistry, vol. 20, pp. 2549-2561, 2010.

[28] N. D. Treat, C. G. Shuttle, M. F. Toney, C. J. Hawker, M. L. Chabinyc, "In Situ Measurement of Power Conversion Efficiency and Molecular Ordering During Thermal Annealing in P3HT:PCBM Bulk Heterojunction Solar Cells," Journal of Materials Chemistry, vol. 21, pp. 15224-15231, 2011.

[29] Y. Ito, A. A. Virkar, S. Mannsfeld, J. H. Oh, M. Toney, J. Locklin, Z. Bao, "Crystalline Ultrasmooth Self-Assembled Monolayers of Alkylsilanes for Organic Field-Effect Transistors," Journal of the American Chemical Society, vol. 131, pp. 9396–9404, 2009.

[30] C. Müller, M. Aghamohammadi, S. Himmelberger, P. Sonar, M. Garriga, A. Salleo, M. C. Quiles, "One-Step Macroscopic Alignment of Conjugated Polymer Systems by Epitaxial Crystallization During Spin-Coating," Advanced Functional Materials, vol. 23, pp. 2368–2377, 2013.

[31] L. Kergoat, N. Battaglini, L. Miozzo, B. Piro, M. C. Pham, A. Yassar, G. Horowitz, "Use of Poly(3-hexylthiophene)/Poly(methyl methacrylate) (P3HT/PMMA) Blends to Improve the Performance of Water-Gated Organic Field-Effect Transistors," Organic Electronics, vol. 12, vol. 1253–1257, 2011.

[32] J. A. Lim, W. H. Lee, H. S. Lee, J. H. Lee, Y. D. Park, K. Cho, " Self-Organization of Ink-jet-Printed Triisopropylsilylethynyl Pentacene via

Evaporation-Induced Flows in a Drying Droplet, "Advanced Functional Materials, vol. 18, pp. 229-234, 2008.

[33] J. Lee, J. Y. Jung, D. H. Kim, J. Y. Kim, B. L. Lee, J. I. Park, J. W. Chung, J. S. Park, B. Koo, Y. W. Jina, S. Lee, "Enhanced Electrical Stability of Organic Thin-Film Transistors with Polymer Semiconductor-Insulator Blended Active Layers," Applied Physics Letters, vol. 100, 083302, 2012.

[34] S. W. Lee, C. H. Kim, S. G. Lee, J. H. Jeong, J. H. Choi, E. S. Lee, " Mobility Improvement of P3HT Thin Film by High-Voltage Electrostatic Field-Assisted Crystallization," Electronic Materials Letters, vol. 9, pp 471-476, 2013.

[35] W. Y. Chou, M. H. Chang, H. L. Cheng, S. P. Yu, Y. C. Lee, C. Y. Chiu, C. Y. Lee and D. Y. Shu, "Application of nanoimprinting technology to organic field-effect transistor," Applied Physics Letters, vol. 96, 083305, 2010.

[36] H. Sirringhaus, R. J. Wilson, R. H. Friend, M. Inbasekaran, W. Wu, E. P. Woo, M. Grell, D. D. C. Bradley, "Mobility Enhancement in Conjugated Polymer Field-Effect Transistors Through Chain Alignment in a Liquid-Crystalline Phase," Applied Physics Letters, vol. 77, 406, 2000.

[37] W. Y. Chou, H. L. Cheng, "An Orientation-Controlled Pentacene Film Aligned by Photoaligned Polyimide for Organic Thin-Film Transistor Applications," Advanced Functional Materials, vol. 14, pp. 811–815, 2004.

[38] M. Aryal, K. Trivedi, W. Hu, "Nano-Confinement Induced Chain Alignment in Ordered P3HT Nanostructures Defined by Nanoimprint Lithography," ACS Nano, vol. 3, pp. 3085–3090, 2009.

[39] B. O'Connor, R. J. Kline, B. R. Conrad, L. J. Richter, D. Gundlach, M. F. Toney, D. M. DeLongchamp, "Anisotropic Structure and Charge Transport in Highly Strain-Aligned Regioregular Poly(3-hexylthiophene)," Advanced Functional Materials, vol. 21, pp. 3697–3705, 2011.

[40] J. H. Oh, W. Y. Lee, T. Noe, W. C. Chen, M. Könemann, and Z. Bao, "Solution-Shear-Processed Quaterrylene Diimide Thin-Film Transistors Prepared By Pressure-Assisted Thermal Cleavage Of Swallow Tails," Journal of the American Chemical Society, vol. 133, pp. 4204-4207, 2011.

[41] Y. Cui, Q. Wei, H. Park, C. M. Lieber, "Nanowire Nanosensors for Highly Sensitive and Selective Detection of Biological and Chemical Species," Science, vol. 293, pp. 1289–1292, 2001.

[42] J. Wang, M. S. Gudiksen, X. Duan, Y. Cui, C. M. Lieber, "Highly Polarized Photoluminescence and Photodetection from Single Indium Phosphide Nanowires," Science 2001, vol. 293, pp. 1455–1457, 2001.

[43] K. Heo, E. Cho, J. Yang, M. Kim, M. Lee, B. Lee, S. Kwon, M. Lee, M. Jo, H. Choi, T. Hyeon, S. Hong, "Large Scale Assembly of Silicon Nanowire Network-Based Devices Using Conventional Microfabrication Facilities," Nano Letters, vol. 8, pp. 4523– 4527, 2008.

[44] F. Kim, S. Kwan, J. Akana, P. Yang , "Langmuir-Blodgett Nanorod Assembly," Journal of the American Chemical Society, vol. 123, pp. 4360-4361, 2001.

[45] S. Jin, D. Whang, M. C. McAlpine, R. S. Friedman, Y. Wu, C. M. Lieber, "Scalable Interconnection and Integration of Nanowire Devices without Registration," Nano Letters, vol. 4, pp. 915–919, 2004.

[46] X. Li, L. Zhang, X. Wang, I. Shimoyama, X. Sun, W. S. Seo, H. Dai, "Langmuir-Blodgett Assembly of Densely Aligned Single-Walled Carbon Nanotubes from Bulk Materials," Journal of the American Chemical Society, vol. 129, pp. 4890–4891, 2007.

[47] G. Yu, A. Cao, C. M. Lieber, "Large-Area Blown Bubble Films of Aligned Nanowires and Carbon Nanotubes," Nature Nanotechnology, vol. 2, pp. 372–377, 2007.

[48] P. A. Smith, C. D. Nordquist, T. N. Jackson, T. S. Mayer, B. R. Martin, J. Mbindyo, T. E. Mallouk, "Electric-Field Assisted Assembly and Alignment of Metallic Nanowires," Applied Physics Letters, vol. 77, pp. 1399–1401, 2000.

[49] O. Englander, D. Christensen, J. Kim, L. Lin, S. J. S. Morris, "Electric-Field Assisted Growth and Self-Assembly of Intrinsic Silicon Nanowires," Nano Letters, vol. 5, pp. 705–708, 2005.

[50] A. Javey, S.W. Nam, R. S. Friedman, H. Yan, C.M. Lieber, "Layerby-Layer Assembly of Nanowires for Three-Dimensional Multifunctional Electronics," Nano Letters, vol. 7, pp. 773–777, 2007.

[51] T. Takahashi, K. Takei, J. C. Ho, Y. Chueh, Z. Fan, A. Javey, "Monolayer Resist for Patterned Contact Printing of Aligned Nanowire Arrays," Journal of the American Chemical Society, vol. 131, pp.2102–2103, 2009.

[52] R. Yerushalmi, Z. A. Jacobson, J. C. Ho, Z. Fan, A. Javey, "Large Scale, Highly Ordered Assembly of Nanowire Parallel Arrays by Differential Roll Printing," Applied Physics Letters, vol. 91, pp. 203104–3, 2007.

[53] L. Wang, M. H. Yoon, G. Lu, Y. Yang, A. Facchetti, T. J. Marks, "High-performance transparent inorganic–organic hybrid thin-filmn-type transistors," Nature Materials, vol. 5, pp. 893-900, 2006.

[54] H. Sirringhaus, P. J. Brown, R. H. Friend, M. M. Nielsen, K. Bechgaard, B. M. W. Langeveld-Voss, A. J. H. Spiering, R. A. J. Janssen, E. W. Meijer, P. Herwig, and D. M. de Leeuw, "Two-Dimensional Charge Transport in Self-Organized, High-Mobility Conjugated Polymers," Nature, vol. 401, pp. 685-688, 1999.

[55] R. J. Kline, M. D. McGehee, E. N. Kadnikova, J. S. Liu, and J. M. J. Frechet, "Controlling the Field-Effect Mobility of Regioregular Polythiophene by Changing the Molecular Weight," Advanced Materials, vol. 15, pp. 1519-1522, 2003.

[56] J. F. Chang, J. Clark, N. Zhao, H. Sirringhaus, D. W. Breiby, J. W. Andreasen, M. M. Nielsen, M. Giles, M. Heeney, and I. McCulloch, "Molecular-Weight Dependence of Interchain Polaron Delocalization and Exciton Bandwidth in High-Mobility Conjugated Polymers," Physical Review B, vol. 74, 115318, 2006.

[57] S. Lenfant, C. Krzeminski, C. Delerue, G. Allan, D. Vuillaume, "Molecular Rectifying Diodes from Self-Assembly on Silicon" Nano Letters, vol. 3, pp. 741-776, 2003.

[58] D. H. Kim, Y. D. Park, Y. Jang, H. Yang, Y. H. Kim, J. I. Han, D. G. Moon, S. Park, T. Chang, C. Chang, M. Joo, C. Y. Ryu, and K. Cho, " Enhancement of Field-Effect Mobility Due to Surface-Mediated Molecular Ordering in Regioregular Polythiophene Thin Film Transistors," Advanced Functional Materials, vol. 15, pp. 77-82, 2005.

[59] S. Cho, K. Leea, J. Yuen, G. Wang, D. Moses, A. J. Heeger, M. Surin, and R. Lazzaroni, "Thermal Annealing-Induced Enhancement of the Field-Effect Mobility of Regioregular Poly(3-hexylthiophene) Films," Japanese Journal of Applied Physics, vol. 100, pp. 114503, 2006.

[60] M. Timo, "Oligomeric and Polymeric Semiconductors Based on Thienothiazoles," E. U. Patents, WO2010115623 A1, 2010.

[61] V. Schmidt, J. V. Wittemann, S. Senz, U. Gösele, "Silicon Nanowires: A Review on Aspects of their Growth and their Electrical Properties," Advanced Materials, vol. 21, pp. 2681–2702, 2009.

[62] R. G. Treuting, S. M. Arnold, "Orientation Habits of Metal Whiskers," Acta Materialia, vol. 5, pp. 598, 1957.

[63] R. S. Wagner, W. C. Ellis, "Vapor-Liquid-Solid Mechanism of Single Crystal Growth," Applied Physics Letters, vol. 4, pp. 89-90, 1964.

[64] E. I. Givargizov, "Fundamental Aspects of VLS growth," Journal of Crystal Growth, vol. 31, pp. 20-30, 1975.

[65] Y. Cui, X. Duan, J. Hu, C. M. Lieber, "Doping and Electrical Transport in Silicon Nanowires," The Journal of Physical Chemistry B, vol. 104, pp.5213-5216, 2000.

[66] T. Y. Tan, N. Li, U. Gösele, "Is there a thermodynamic size limit of nanowires grown by the vapor-liquid-solid process," Applied Physics Letters, vol. 83, pp. 1199-1201, 2003.

[67] V. Schmidt, J. V. Wittemann, S. Senz, U. Gösele, "Silicon Nanowires: A Review on Aspects of their Growth and their Electrical Properties" Advanced Materials, vol. 21, pp. 2681–2702, 2009.

[68] K. Ogata, E. Sutter, X. Zhu, S. Hofmann, "Ni-silicide growth kinetics in Si and Si/SiO_2 core/shell nanowires," Nanotechnology, vol. 22, pp. 365305-365313, 2011.

[69] 胡文平，有機場效應晶體管，一版，北京，科學出版社，西元二零一一年。

[70] S. E. Oraby, A. M. Alaskari, "Atomic Force Microscopy (AFM) Topographical Surface Characterization of Multilayer-Coated and Uncoated Carbide Inserts," World Academy of Science, Engineering and Technology 46, 2010.

[71] 中國化工企業聯盟, "112-04-9 Octadecyltrichlorosilane" www.chem960.com/cas/112-04-9.html

[72] J&K Scientific Ltd, "n-Octyltrichlorosilane," www.jk-scientific.com/EN/products/J20S12750.html

[73] S. A. DiBenedetto, A. Facchetti, M. A. Ratner, T. J. Marks, "Molecular Self-Assembled Monolayers and Multilayers for Organic and Unconventional Inorganic Thin-Film Transistor Applications," Advance Materials, vol. 21, pp. 1407–1433, 2009.